

An asymptotic safety scenario for gauged chiral Higgs-Yukawa models

Holger Gies,^{1,*} Stefan Rechenberger,^{2,3,†} Michael M. Scherer,^{4,‡} and Luca Zambelli^{1,5,§}

¹*Theoretisch-Physikalisches Institut, Friedrich-Schiller-Universität Jena, D-07743 Jena, Germany*

²*Institut für Physik, Johannes-Gutenberg-Universität Mainz, D-55099 Mainz, Germany*

³*Faculty of Science (IMAPP), Radboud University Nijmegen, NL-6500 GL Nijmegen, The Netherlands*

⁴*Institut für Theoretische Physik, Universität Heidelberg, D-69120 Heidelberg, Germany*

⁵*Dip. di Fisica, Università degli Studi di Bologna, INFN Sez. di Bologna via Irnerio 46, I-40126 Bologna, Italy*

We investigate chiral Higgs-Yukawa models with a non-abelian gauged left-handed sector reminiscent to a sub-sector of the standard model. We discover a new weak-coupling fixed-point behavior that allows for ultraviolet complete RG trajectories which can be connected with a conventional long-range infrared behavior in the Higgs phase. This non-trivial ultraviolet behavior is characterized by asymptotic freedom in all interaction couplings, but a quasi conformal behavior in all mass-like parameters. The stable microscopic scalar potential asymptotically approaches flatness in the ultraviolet, however, with a non-vanishing minimum increasing inversely proportional to the asymptotically free gauge coupling. This gives rise to nonperturbative – though weak-coupling – threshold effects which induce ultraviolet stability along a line of fixed points. Despite the weak-coupling properties, the system exhibits non-Gaussian features which are distinctly different from its standard perturbative counterpart: e.g., on a branch of the line of fixed points, we find linear instead of quadratically running renormalization constants. Whereas the Fermi constant and the top mass are naturally of the same order of magnitude, our model generically allows for light Higgs boson masses. Realistic mass ratios are related to particular RG trajectories with a “walking” mid-momentum regime.

I. INTRODUCTION

The chiral, gauge and flavor structures of the standard model lie at the heart of its greatest successes. At the same time, they also mark its fundamental deficits: the chiral structure requires a scalar Higgs field which suffers from a severe triviality problem, suggesting that the conventional Higgs sector is not a fundamental quantum field theory [1]. Also the product structure of the gauge symmetry involves a U(1) gauge symmetry which has a similar (though less pressing) triviality problem [2–5]. In addition, the perturbative running of the Higgs sector appears to require unnaturally fine-tuned initial conditions in order to separate the electroweak scale from the Planck or GUT-like scales. In the same spirit, the diversity of scales in the flavor sector so far has not found a convincing natural explanation.

Whereas many attempts to resolve these deficits are built on postulating new degrees of freedom, new symmetries or new quantization rules, we wish to take a fresh look at conventional systems within quantum field theory, relying on the degrees of freedom already observed in experiments. In the present work, we even consider a reduced model involving a chiral Higgs-Yukawa system with a non-abelian gauged left-handed sector, which can be viewed as the scalar Higgs-sector chirally coupled to a top-bottom fermion sector and a left-handed SU(N_L) gauge group. Many aspects of the weak-coupling behav-

ior of this model are straightforwardly accessible in perturbation theory, showing some indications of the structural deficits mentioned above for the standard model, in particular, the triviality and the hierarchy problem of the Higgs sector.

In the present work, we therefore explore the model using the functional renormalization group (RG) as a non-perturbative method. Whereas all perturbative physics still remains included, we can specifically address non-perturbative features to which naive perturbation theory is completely blind. In fact, one such potentially important feature in this context are threshold phenomena as has been pointed out in [6, 7]. Threshold effects such as the decoupling of massive modes is non-perturbative in the sense that dynamically generated masses can be proportional to the coupling. A decoupling that proceeds, for instance, inversely proportional to some power of the mass therefore cannot have a naive perturbative Taylor expansion in powers of the coupling without spoiling the physical threshold behavior at any finite order of this expansion. It is important to emphasize that this statement holds independently of the coupling strength. In fact, the threshold phenomena relevant for the present work turn out to be active in the weak-coupling region of the model. In particular, the gauge interactions are fully in the domain of asymptotic freedom. Of course, methods to deal with threshold phenomena have also been developed within perturbative approaches [8] and are commonly used to follow the RG evolution in the standard model [9]. Hence, we expect that our results should also be reproducible within a perturbative treatment that properly accounts for threshold effects, for instance, in a mass-dependent RG scheme.

The scenario developed in the present work builds on

*Electronic address: holger.gies@uni-jena.de

†Electronic address: rechenbe@uni-mainz.de

‡Electronic address: m.scherer@thphys.uni-heidelberg.de

§Electronic address: luca.zambelli@uni-jena.de

the concept of asymptotic safety [10] which is a generalization of asymptotic freedom to non-Gaussian, i.e. interacting, UV fixed points. A quantum field theory can be UV complete if its RG trajectory approaches a fixed point in the UV, such that a UV cutoff Λ can be sent to infinity, $\Lambda \rightarrow \infty$. Though standard perturbative renormalizability is included in this scenario if the fixed point occurs at zero coupling, it is not mandatory for UV completeness, but is merely a criterion for the applicability of perturbation theory. Asymptotically safe theories are well known and understood in lower-dimensional fermionic systems [11–14]. Most prominently, asymptotic safety has by now become an established scenario for a UV complete quantum theory of gravity [15]. In this larger context of asymptotically safe gravity, new fixed point structures can also arise in the combined gravity-scalar [16], gravity-Yukawa [17], gravity-fermion [18], or gravity-photon [19] sector, potentially curing the UV problems of the standard model.

The present work continues the search for asymptotically safe Yukawa models initiated in [6, 7]. However, our new findings including a gauge sector go beyond those scenarios, as the near-conformal behavior required for a non-Gaussian fixed point does not occur in the couplings and the vacuum expectation value, but is shifted to the mass parameters of the model in the Higgs regime. This gives rise to a novel and unconventional asymptotic safety scenario for gauged Higgs-Yukawa systems which could be active in the electroweak sector of the standard model. If so, such a scenario not only modifies the UV behavior of the standard model potentially curing some deficits, but may also have implications for the infrared behavior. For instance, the accessible space of mass and coupling parameters can be constrained as a result of the RG flow. First results along this line will be discussed below.

The article is organized as follows. In Sect. II, we motivate the model in the context of earlier work, emphasizing the fact that the construction of an asymptotically safe scenario for the standard model Higgs sector appears to favor a chiral gauge structure. Section III details the application of the functional RG technique to the present problem and summarizes our results for the RG flow equations evaluated to next-to-leading order in a derivative expansion of the Higgs-Yukawa system. The fixed point structure of the model facilitating an asymptotic safety scenario is analyzed in Sect. IV, revealing a line of fixed points with suitable UV properties. We explicitly verify in Sect. V that the UV fixed points can be connected with the Higgs phase of the model, such that the IR properties are qualitatively reminiscent to those of the standard model. This demonstrates that the present chiral gauged Higgs-Yukawa model can be a UV complete quantum field theory. Conclusions are presented in Sect. VI, and many important details of the calculations are deferred to the appendices.

II. MOTIVATION OF THE MODEL

The chiral gauged Higgs-Yukawa model investigated in the present work can, of course, straightforwardly be motivated from the (experimentally observed) Higgs sector of the standard model. However, it is instructive to realize that also purely theoretical arguments for the construction of an asymptotically safe Higgs-Yukawa system lead to the same model in a natural way.

Inspired by the asymptotic safety of fermionic models such as the simple Gross-Neveu model in $2 < d < 4$ dimensions [11, 12], it is tempting to ask, whether this non-perturbative renormalizability at a non-Gaussian fixed point can also be extended to $d = 4$ dimensions [20–22]. Even though final answers in complex models have not been given so far, simple toy models such as the Gross-Neveu model with a discrete \mathbb{Z}_2 symmetry show a vanishing of the required fixed points in the limit $d \rightarrow 4$ (more precisely: the non-Gaussian fixed point typically merges with the Gaussian fixed point for $d \rightarrow 4$) [12] as is also suggested by lattice simulations [23].

Moreover, since purely fermionic models and Yukawa models with similar mass generating phase transitions are typically in the same universality class [24, 25], it is reasonable to treat the fermionic and the bosonic degrees of freedom on the same footing, i.e., both as fundamental.

An extensive exploration of the simple \mathbb{Z}_2 -invariant Yukawa model using the functional RG [6] has provided evidence that (i) no non-Gaussian fixed point exists in the symmetric regime, whereas (ii) the symmetry-broken regime can give rise to suitable fixed points, provided the symmetry-breaking condensate approaches a fixed point and behaves nearly conformal. If this conformal condensate behavior sets in, a threshold behavior is induced that can naturally lead to a balancing of interactions up to the highest scales. More concretely, the flow of the scalar vacuum expectation value (vev) \bar{v} can be parametrized by the dimensionless combination $\kappa = v^2/(2k^2)$, the β function of which has the generic structure

$$\partial_t \kappa \equiv \partial_t \frac{v^2}{2k^2} = -2\kappa + \text{boson fluct.} - \text{fermion fluct.}, \quad (1)$$

where $\partial_t = k \frac{d}{dk}$ and k denotes an RG scale. In order to induce a non-Gaussian fixed point at positive $\kappa_* > 0$, facilitating a (near) conformal condensate behavior $v \sim k$, the bosons obviously have to dominate over the fermion fluctuations due to the relative minus sign. Whether or not this is the case essentially depends on the number of degrees of freedom of the model. The analysis of [6] containing one real scalar field and N_f Dirac fermions revealed that the necessary bosonic dominance occurs only for an unphysical value of $N_f \lesssim 0.3$.

An elegant way to enhance the boson fluctuations (without unnaturally increasing the number of boson fields) was identified in [7]: chiral Yukawa couplings of N_L complex scalar fields ϕ^a with N_L left-handed fermions ψ_L^a and a single right-handed fermion ψ_R leads to an $\sim N_L$ enhancement of the boson fluctuations whereas the

fermion fluctuations remain of $\sim \mathcal{O}(1)$. This is already a first indication that asymptotically safe scenarios prefer chiral Yukawa systems. In [7], suitable non-Gaussian fixed points were discovered for a wide range of N_L including $N_L = 2$ in a leading-order derivative expansion analysis. Moreover, one of the admissible fixed points has only one UV-attractive direction, thus implying that only one physical parameter has to be fixed, e.g., the vev $v = 246\text{GeV}$, whereas all other IR quantities such as the Higgs or the top mass would be a pure prediction of the theory.

However, these suitable fixed points apparently get destabilized at next-to-leading order in the derivative expansion [7] for a physical reason: the derivative expansion assumes that field amplitudes remain sufficiently slowly varying at a given RG scale during the flow. But in the chiral Yukawa model, massless Goldstone modes occur in the broken regime which together with the massless bottom-type fermions of the model induce strong contributions which are not damped by threshold effects. We expect this argument to be rather generic: non-Gaussian threshold-induced fixed points in Yukawa models with continuous symmetries are likely to be destabilized by massless Goldstone modes in the broken regime.

There is one particular mechanism to avoid massless Goldstone modes in systems with broken continuous symmetries: the Higgs mechanism [26]. Hence, the search for non-Gaussian fixed points in Yukawa systems naturally leads us to the inclusion of a chiral gauge sector in our model. In addition to “eating up” the scalar Goldstone modes, we expect the gauge bosons to also contribute in a beneficial way to the stabilization of the scalar condensate, cf. Eq. (1).

On the other hand, already at this point, we can expect that the picture of the conformal threshold behavior might be modified upon the inclusion of gauge fields. The reason is that non-abelian gauge theories are asymptotically free. Whereas for any finite value of the gauge coupling g^2 , we may find stable non-Gaussian fixed points along the lines of [6, 7], the UV limit where $g^2 \rightarrow 0$ must ultimately leave its imprints also in the Yukawa sector. It is one of the main results of the present work that the conformal threshold behavior indeed persists, however not in the form of near-conformal condensate and couplings, but in the form of near-conformal mass parameters.

The reasoning of this section leads us to consider chiral gauged Higgs-Yukawa models with a standard classical action of the form (here and in the following, we work in Euclidean space)

$$S_{\text{cl}} = \int d^d x \left[\frac{1}{4} F_{\mu\nu}^i F^{i\mu\nu} + (D^\mu \phi)^\dagger (D_\mu \phi) + \bar{m}^2 \rho + \frac{\bar{\lambda}}{2} \rho^2 + i(\bar{\psi}_L^a \not{D}^{ab} \psi_L^b + \bar{\psi}_R \not{D} \psi_R) + \bar{h} \bar{\psi}_R \phi^{\dagger a} \psi_L^a - \bar{h} \bar{\psi}_L^a \phi^a \psi_R \right] \quad (2)$$

where $\rho := \phi^{\dagger a} \phi^a$. The classical parameter space is spanned by the boson mass \bar{m} , the scalar self-interaction

$\bar{\lambda}$, the Yukawa coupling \bar{h} and the gauge coupling \bar{g} which occurs in the covariant derivatives for the matter fields in the fundamental representation of the gauge group ($a, b, \dots = 1, \dots, N_L$),

$$D_\nu^{ab} = \partial_\nu \delta^{ab} - i\bar{g} W_\nu^i (T^i)^{ab}, \quad (3)$$

where W_ν^i denotes the Yang-Mills vector potential. The fermionic field content consists of a left-handed N_L -plet (e.g., a top-bottom doublet for $SU(N_L = 2)$) and one right-handed fermion (e.g., the right-handed top-quark component); right-handed bottom-type components are not considered, such that only the top quark can become massive upon symmetry breaking. The fermions are considered to occur in N_g generations; the generation structure does not have any nontrivial interplay with the gauge or scalar sector, such that the corresponding generation index is suppressed. The general calculations of the present work in principle hold for any simple Lie group, hence we keep the notation general. In concrete calculations we will confine ourselves to $SU(N_L = 2)$. We expect the mechanisms presented below to hold for any gauge group.¹ The generators of the gauge group satisfy the corresponding algebra, $[T^i, T^j] = i f^{ijk} T^k$ with structure constants f^{ijk} , and the nonabelian field strength in Eq. (2) is given by $F_{\mu\nu}^i = \partial_\mu W_\nu^i - \partial_\nu W_\mu^i + \bar{g} f^{ijl} W_\mu^j W_\nu^l$, where i, j, k, \dots denote adjoint indices. For the scalar potential, we only consider the invariant $\rho := \phi^{\dagger a} \phi^a$. For later convenience, we remark that the complex scalar field can equally well be expressed in terms of $2N_L$ real scalar fields,

$$\phi^a = \frac{1}{\sqrt{2}}(\phi_1^a + i\phi_2^a), \quad \phi^{a\dagger} = \frac{1}{\sqrt{2}}(\phi_1^a - i\phi_2^a), \quad (4)$$

where $\phi_1^a, \phi_2^a \in \mathbb{R}$. In addition to the local gauge symmetry, the model is invariant under a global $U(1)_L \times U(1)_R$ symmetry, where the fermions transform under their corresponding chiral component and the scalar transforms under both with opposite charges. If the gauge symmetry is chosen to be $SU(N_L)$, its global part and the $U(1)_L$ are subgroups of a global $U(N_L)_L$ symmetry. In the following, we will analyze the RG flow of generic effective actions in a theory space inspired by the classical action given in Eq. (2) and its symmetries.

¹ Of course, the present model has perturbative gauge anomalies for $SU(N_L \geq 3)$ [27]. For $SU(N_L = 2)$ or $SP(N_L)$, the model has a global Witten anomaly for odd N_g [28]. In these anomalous cases, the model cannot be a consistent quantum field theory as it stands. The RG flows determined below should in such cases be viewed as a projection of a larger (unspecified) anomaly-free model, e.g., the standard model with only one generation, onto an effectively reduced theory subspace.

III. RG FLOW OF THE MODEL

A. Functional RG

In the present work, we study the chiral gauged Higgs-Yukawa model using the functional RG. More precisely, we study the RG flow of effective action functionals Γ_k that are spanned by the same field content and the same symmetries as Eq. (2). Here, the scale k denotes an IR cutoff parametrizing those fluctuations with momenta $p^2 \lesssim k^2$ that still have to be fully integrated out to arrive at the full effective action $\Gamma = \Gamma_{k \rightarrow 0}$. The latter corresponds to the standard generating functional of 1PI correlation functions encoding the physical properties of the theory.

The set of functionals Γ_k hence defines a one-parameter family of effective actions that relate the physical long-range behavior for $k \rightarrow 0$ with a microscopic action functional at $k \rightarrow \Lambda$, where Λ denotes a microscopic UV scale, such that Γ_Λ is related to the ‘‘classical action to be quantized’’. The trajectory interconnecting all these scales is determined by the Wetterich equation [29]

$$\partial_t \Gamma_k[\Phi] = \frac{1}{2} \text{STr} \{ [\Gamma_k^{(2)}[\Phi] + R_k]^{-1} (\partial_t R_k) \}. \quad (5)$$

Here $\Gamma_k^{(2)}$ is the Hessian, i.e., the second functional derivative with respect to the field Φ , representing a collective field variable for all bosonic or fermionic degrees of freedom. The momentum-dependent regulator function R_k encodes the suppression of IR modes below a momentum scale k , for reviews see [30, 31].

Whereas Eq. (5) in conventional applications is solved subject to an initial condition $S_\Lambda \simeq S_{\text{cl}}$ (the bare action), we use the flow equation also to search for suitable initial conditions in the vicinity of UV attractive fixed points. If such fixed points exist, trajectories can be constructed that are UV complete by approaching and ultimately hitting the fixed point in the limit $\Lambda \rightarrow \infty$. The corresponding system together with its flow to the IR represents a quantum field theory which can be valid on all scales.

For the present work, the crucial property of the functional RG evolution is the fact that the computation of correlation functions involves the exact (regularized) propagator at a scale k given by $[\Gamma_k^{(2)}[\Phi] + R_k]^{-1}$ in Eq. (5). Especially, if a dynamically generated mass exists at some scale k , it is included as a corresponding gap in the self-energy. By contrast, naive perturbation theory consists of an expansion about zero coupling which is blind to dynamically generated masses. Of course, the latter can be included in a reorganized perturbative expansion, but the functional RG does so in a self-consistent and RG-improved manner. In this way, we can particularly well deal with the threshold regime where the mass generation sets in dynamically.

As we are dealing with a gauge theory, the RG flow has to be constructed such that gauge symmetry is preserved. As in standard continuum calculations, gauge

fixing is required such that gauge symmetry is encoded in constraints (generalized Ward identities). While it is by now well understood how to deal with this issue in the non-perturbative strong-coupling domain [30, 32–36], the present work only requires the weak-coupling limit of the gauge sector essentially on a one-loop level. For this, we will use the standard background field formalism [37]; details of this part of the calculation can be found in App. C 1.

In the following, we use the R_α gauge (or its background-field variant for the computation of the gauge sector, see App. C 1). For its definition in the present context, let us first decompose the scalar field into the bare vev \bar{v} and the fluctuations $\Delta\phi$ about the vev

$$\phi^a = \frac{\bar{v}}{\sqrt{2}} \hat{n}^a + \Delta\phi^a, \quad \Delta\phi^a = \frac{1}{\sqrt{2}} (\Delta\phi_1^a + i\Delta\phi_2^a), \quad (6)$$

where \hat{n} is a unit vector ($\hat{n}^\dagger \hat{n}^a = 1$) defining the direction of the vev in fundamental Yang-Mills space. Then, the gauge fixing condition is given by

$$G^i(W) = \partial_\mu W_\mu^i + i\alpha \bar{v} \bar{g} (T_{\hat{n}\check{a}}^i \Delta\phi_1^{\check{a}} + iT_{\hat{n}a}^i \Delta\phi_2^a) = 0, \quad \check{a} \neq \hat{n}, \quad (7)$$

where α is a gauge-fixing parameter interpolating between the unitary gauge at $\alpha \rightarrow \infty$ and the Landau gauge at $\alpha \rightarrow 0$. Here and in the following, the label \hat{n} in place of that index with the unit vector \hat{n} (or \hat{n}^\dagger , depending on the position of the index). In Eq. (7) the component $\Delta\phi_1^{\hat{n}}$ is not included in the sum over \check{a} . This implies that the gauge fixing only involves the Goldstone-boson directions and not the radial mode. The gauge fixing is implemented by including a gauge-fixing term in the action

$$S_{\text{gf}} = \frac{1}{2\alpha} \int d^d x G^i(W) G^i(W),$$

as well as a Faddeev-Popov term localized in terms of ghost fields c^i and \bar{c}^i with a bare action

$$S_{\text{gh}} = \int d^d x \bar{c}^i \mathcal{M}^{ij} c^j.$$

The Faddeev-Popov operator is given by

$$\mathcal{M}^{ij} = -\partial^2 \delta^{ij} - \bar{g} f^{ilj} \partial_\mu W^{l\mu} + \sqrt{2} \alpha \bar{v} \bar{g}^2 T_{\hat{n}\check{a}}^i T_{\check{a}b}^j \Delta\phi^b, \quad (8)$$

again excluding $a = \hat{n}$ in the sum over \check{a} .

With these preparations, we can now write down the space of action functionals considered in this work:

$$\begin{aligned} \Gamma_k = \int d^d x & \left[U(\rho) + Z_\phi (D^\mu \phi)^\dagger (D_\mu \phi) \right. \\ & + i(Z_L \bar{\psi}_L^a \not{D}^{ab} \psi_L^b + Z_R \bar{\psi}_R \not{D} \psi_R) \\ & + \bar{h} \bar{\psi}_R \phi^{a\dagger} \psi_L^a - \bar{h} \bar{\psi}_L^a \phi^a \psi_R \\ & \left. + \frac{Z_W}{4} F_{\mu\nu}^i F^{i\mu\nu} + \frac{Z_\phi}{2\alpha} G^i G^i - \bar{c}^i \mathcal{M}^{ij} c^j \right]. \quad (9) \end{aligned}$$

All couplings, wave function renormalizations $Z_{\phi,L,R,W}$ and the effective scalar potential $U(\rho)$ are taken to be k dependent. The scalar sector corresponds to a next-to-leading order derivative expansion of the action. In addition, the flows of the Yukawa coupling, the gauge coupling and the wave function renormalizations are evaluated in the presence of a k -dependent minimum of the potential in order to properly account for the threshold phenomena.

As Eq. (9) already indicates, we ignore any nontrivial running of the ghost sector and of the gauge parameter α and drop any higher order gauge-field operators, as this is not necessary for an exact flow of the gauge coupling at one-loop order. For the actual computation of the latter using the background field method, the ordinary derivatives in the gauge fixing and ghost terms are replaced by covariant derivatives \bar{D} w.r.t. the background field \bar{W} , cf. App. C 1. The Yukawa sector remains however unaffected by the background field.

To sum up, the subset of theory space we are considering is parametrized by Z_ϕ , Z_L , Z_R , Z_W , \bar{h} , \bar{v} and all the parameters contained in U different from \bar{v} itself. (The running of the gauge coupling \bar{g} in the background field method is related to the wave function renormalization Z_W , see below).

It is also useful to introduce a simplifying notation for the masses in the symmetry-broken regime, which are directly related to the parameters listed above. The (unrenormalized) mass matrix for the gauge bosons is given by

$$\bar{m}_W^2{}^{ij} = \frac{1}{2} Z_\phi \bar{g}^2 \bar{v}^2 \{T^i, T^j\}_{\hat{n}\hat{n}}. \quad (10)$$

Since it is diagonalizable, we can choose a basis in adjoint color space where

$$\bar{m}_W^2{}^{ij} = \bar{m}_{W,i}^2 \delta^{ij} \quad (\text{no sum over } i). \quad (11)$$

The scalar mass matrix reads

$$\bar{m}_\phi^2{}^{ab} = \bar{v}^2 U'' \left(\frac{\bar{v}^2}{2} \right) \hat{n}^a \hat{n}^{\dagger b}.$$

In a diagonalizing basis, we have $\bar{m}_\phi^2{}^{ab} = \bar{m}_{\phi,a}^2 \delta^{ab}$ (no sum over a), with, of course, vanishing eigenvalues for the would-be Goldstone modes corresponding to the broken generators in this gauge. Furthermore the (unrenormalized) ‘‘top mass’’ i.e. the mass of the $\psi^{\hat{n}}$ mode, is given by

$$\bar{m}_t = \frac{\bar{h}\bar{v}}{\sqrt{2}}. \quad (12)$$

The corresponding renormalized quantities include appropriate factors of the wave function renormalizations, see below. Incidentally, the above reasoning for identifying the particle spectrum follows that used in straightforward perturbative considerations. We emphasize that a proper gauge- and scheme-independent identification requires careful nonperturbative considerations, see e.g. [38, 39].

B. Dimensionless variables

Whereas the long-range observables are dimensionful quantities expressed, for instance, in terms of an absolute measurement scale, the search for UV fixed points requires dimensionless variables. If the system approaches a conformal behavior, it is expected to become self-similar, i.e., to look the same independently of the measurement scale. Also the flow equations can conveniently be expressed in terms of dimensionless renormalized variables. For this, we define the corresponding Yukawa and gauge couplings,

$$h^2 = \frac{k^{d-4} \bar{h}^2}{Z_\phi Z_L Z_R}, \quad g^2 = \frac{\bar{g}^2}{Z_W k^{4-d}}, \quad (13)$$

as well as the dimensionless effective potential

$$u(\tilde{\rho}) = k^{-d} U(Z_\phi^{-1} k^{d-2} \tilde{\rho}), \quad \tilde{\rho} = \frac{Z_\phi \rho}{k^{d-2}}. \quad (14)$$

The effective potential is expressed in terms of the dimensionless renormalized field variable $\tilde{\rho}$. If the system is in the spontaneously symmetry-broken (SSB) regime, we use the dimensionless renormalized minimum of the potential,

$$\kappa = \frac{Z_\phi \bar{v}^2}{2k^{d-2}} = \tilde{\rho}_{\min}. \quad (15)$$

Correspondingly, an expansion of the effective potential about the minimum can be useful in the SSB regime,

$$\begin{aligned} u &= \sum_{n=2}^{N_p} \frac{\lambda_n}{n!} (\tilde{\rho} - \kappa)^n \\ &= \frac{\lambda_2}{2!} (\tilde{\rho} - \kappa)^2 + \frac{\lambda_3}{3!} (\tilde{\rho} - \kappa)^3 + \dots \end{aligned} \quad (16)$$

In the symmetric regime where $\tilde{\rho}_{\min} = 0$, we use the expansion

$$u = \sum_{n=1}^{N_p} \frac{\lambda_n}{n!} \tilde{\rho}^n = m^2 \tilde{\rho} + \frac{\lambda_2}{2!} \tilde{\rho}^2 + \frac{\lambda_3}{3!} \tilde{\rho}^3 + \dots \quad (17)$$

Note that the expansion coefficients λ_n in Eqs. (16) and (17) are generally not identical in the two different regimes; also their flow will be different. Still the standard ϕ^4 coupling in both cases is related to λ_2 . The contribution of the field renormalizations deviating from canonical scaling is encoded in the scale-dependent anomalous dimensions

$$\begin{aligned} \eta_\phi &= -\partial_t \log Z_\phi, & \eta_W &= -\partial_t \log Z_W \\ \eta_L &= -\partial_t \log Z_L, & \eta_R &= -\partial_t \log Z_R. \end{aligned}$$

Setting the anomalous dimensions to zero defines the leading-order derivative expansion. At next-to-leading order, it is important to distinguish between the running

of Z_L and that of Z_R as they acquire different loop contributions, see below.

As we compute the running of the gauge coupling with the background-field method, we can make use of the fact that the product of bare coupling and bare background gauge field $\bar{g}W_\mu^a$ is a renormalization group invariant combination in the background-field gauge. Therefore, the running of the gauge coupling is tightly linked to that of the background-field renormalization [37], implying that

$$\beta_{g^2} = \partial_t g^2 = (d - 4 + \eta_W)g^2. \quad (18)$$

For an analysis of the threshold behavior of the system, also the dimensionless renormalized mass parameters turn out to be useful:

$$\mu_{W,i}^2 = \frac{\bar{m}_{W,i}^2}{Z_W k^2}, \quad \mu_{\phi,a}^2 = \frac{\bar{m}_{\phi,a}^2}{Z_\phi k^2}, \quad \mu_t^2 = \frac{\bar{m}_t^2}{Z_L Z_R k^2}. \quad (19)$$

From a general perspective, the dimensionless renormalized formulation can only implicitly depend on our RG scale k , as the latter is dimensional. Therefore, a fixed point associated with conformal behavior corresponds to the vanishing of the β functions of all dimensionless variables. However, the above given list of dimensionless couplings contains some redundancy, as, for instance, the dimensionless top mass is related to the Yukawa coupling and the potential minimum, and similarly for the gauge boson and Higgs masses. A more precise statement thus is that a fixed point exists, if the β functions for a complete linearly independent set of dimensionless variables vanish. For the moment, we keep this redundancy of variables in order to determine a suitable choice of variables below.

As we will specialize to the case of $SU(N_L = 2)$ below, let us already list here the relations between all couplings for this case:

$$\mu_W^2 = \frac{1}{2}g^2\kappa, \quad \mu_H^2 = 2\lambda_2\kappa, \quad \mu_t^2 = \kappa h^2. \quad (20)$$

The dimensional renormalized masses of the system can straightforwardly be obtained by trivial multiplication

with the scale,

$$m_W^2 = \mu_W^2 k^2, \quad m_H^2 = \mu_H^2 k^2, \quad m_t^2 = \mu_t^2 k^2. \quad (21)$$

Together with the dimensionful renormalized vev,

$$v = \sqrt{2\kappa} k^{(d-2)/2} \equiv Z_\phi^{1/2} \bar{v}, \quad (22)$$

this list constitutes our long-range observables to be computed from the flow towards the IR.

C. Flow equations for the matter couplings

Large parts of the calculation of the flow equation in the matter sector can be done in arbitrary Euclidean space dimension d , for any number of left-handed fermion components N_L , number of generations N_g and any gauge group with a corresponding dimension d_{ad} of its adjoint representation (e.g., $d_{\text{ad}} = N_L^2 - 1$ for $SU(N_L)$). Furthermore, the dimension of the representation of the Clifford algebra for the chiral fermions will be abbreviated by d_γ . As a special case, we have chosen to work in Landau gauge $\alpha \rightarrow 0$ (or Landau-DeWitt gauge for the background-field part) for reasons of simplicity. Also, Landau gauge is known to be a fixed point of the RG flow [40] and hence is a self-consistent choice.

Later on, we specialize to $d = 4$, $SU(N_L = 2)$ with $d_{\text{ad}} = 3$ and $d_\gamma = 2$. Also, we use the linear regulator that is optimized for the present truncation [41]. We have not found any indication that the qualitative features described below depend on any of these concrete choices.

We defer the details of the calculation as well as the properties of the threshold functions l, m, a occurring below with various sub- and superscripts and parametrizing the decoupling of massive modes to App. A 2.

Let us start with the flow of the effective potential which is driven by scalar (B superscript), Dirac fermion (F), left-handed Weyl fermion (L), as well as gauge boson (G) and ghost (gh) fluctuations. Introducing the abbreviation $v_d = 1/(2^{d+1}\pi^{d/2}\Gamma(d/2))$ the flow of the potential is described by

$$\begin{aligned} \partial_t u = & -du + (d - 2 + \eta_\phi)\tilde{\rho}u' + 2v_d \left\{ -2d_{\text{ad}}l_0^{(\text{gh})d}(0) + \sum_{i=1}^{d_{\text{ad}}} \left[(d-1)l_{0T}^{(G)d}(\mu_{W,i}^2(\tilde{\rho})) + l_{0L}^{(G)d}(0) \right] \right. \\ & \left. + (2N_L - 1)l_0^{(B)d}(u') + l_0^{(B)d}(u' + 2\tilde{\rho}u'') - d_\gamma N_g \left[(N_L - 1)l_0^{(L)d}(0) + 2l_0^{(F)d}(\tilde{\rho}h^2) \right] \right\}. \end{aligned} \quad (23)$$

where $\mu_{W,i}^2(\tilde{\rho})$ are defined as functions of the full scalar field in analogy with Eqs. (10),(11), reducing to the dimensionless gauge boson renormalized masses for $\tilde{\rho} = \kappa$. The full flow of u (23) can be used to extract the flows of

the coefficients of the potential expansions Eqs. (16),(17) in both regimes. For the flow of the minimum κ in the SSB regime, we use the fact that the first derivative of u

vanishes at the minimum, $u'(\kappa) = 0$. This implies

$$\begin{aligned} 0 &= \partial_t u'(\kappa) = \partial_t u'(\tilde{\rho})|_{\tilde{\rho}=\kappa} + (\partial_t \kappa) u''(\kappa) \\ \Rightarrow \partial_t \kappa &= -\frac{1}{u''(\kappa)} \partial_t u'(\tilde{\rho})|_{\tilde{\rho}=\kappa}. \end{aligned} \quad (24)$$

Whereas the flow in the symmetric regime is unambiguous, a subtlety arises in the SSB regime: here, the flow of the Yukawa coupling and the scalar anomalous dimension for the would-be Goldstone modes can, in principle, be different from those of the radial mode. As the Goldstone

modes as such are not present in the standard model, we compute the Yukawa coupling and the scalar anomalous dimension by projecting the flow onto the radial scalar operators in the SSB regime. Note that this strategy is different from that used for critical phenomena in other Yukawa or bosonic systems, where the Goldstone modes typically dominate criticality. Accordingly, the flow of the Yukawa coupling h can be derived and we find the same result already presented in [7], that is

$$\begin{aligned} \partial_t h^2 &= (d-4 + \eta_\phi + \eta_L + \eta_R) h^2 + 4v_d h^4 \left\{ (2\tilde{\rho}u'') l_{1,2}^{(\text{FB})d}(\tilde{\rho}h^2, u') - (6\tilde{\rho}u'' + 4\tilde{\rho}^2 u''') l_{1,2}^{(\text{FB})d}(\tilde{\rho}h^2, u' + 2\tilde{\rho}u'') \right. \\ &\quad \left. - l_{1,1}^{(\text{FB})d}(\tilde{\rho}h^2, u') + l_{1,1}^{(\text{FB})d}(\tilde{\rho}h^2, u' + 2\tilde{\rho}u'') + (2\tilde{\rho}h^2) l_{2,1}^{(\text{FB})d}(\tilde{\rho}h^2, u') - (2\tilde{\rho}h^2) l_{2,1}^{(\text{FB})d}(\tilde{\rho}h^2, u' + 2\tilde{\rho}u'') \right\}_{\tilde{\rho}=\tilde{\rho}_{\min}} \end{aligned} \quad (25)$$

Note that the whole expression in curly braces vanishes in the symmetric regime where $\tilde{\rho} = 0$. Also, we observe that no gauge contributions to the running of this coupling occur which is a special feature of Landau gauge; a brief explanation of this fact is given in App. B. Finally, the anomalous dimensions read

$$\begin{aligned} \eta_\phi &= \frac{8v_d}{d} \left\{ \tilde{\rho}(3u'' + 2\tilde{\rho}u''')^2 m_{2,2}^{(\text{B})d}(u' + 2\tilde{\rho}u'', u' + 2\tilde{\rho}u'') + (2N_L - 1) \tilde{\rho}u''^2 m_{2,2}^{(\text{B})d}(u', u') \right. \\ &\quad \left. + d_\gamma N_g h^2 \left[m_4^{(\text{F})d}(\tilde{\rho}h^2) - \tilde{\rho}h^2 m_2^{(\text{F})d}(\tilde{\rho}h^2) \right] \right\} \\ &\quad + \frac{8v_d(d-1)}{d} \left\{ -2g^2 \sum_{a=1}^{N_L} \sum_{i=1}^{d_{\text{ad}}} T_{\hat{n}a}^i T_{a\hat{n}}^i l_{1,1}^{(\text{BG})d}(u', \mu_{W,i}^2) + \sum_{i=1}^{d_{\text{ad}}} \frac{\mu_{W,i}^4}{\tilde{\rho}} \left[2a_1^d(\mu_{W,i}^2) + m_2^{(\text{G})d}(\mu_{W,i}^2) \right] \right\}_{\tilde{\rho}=\tilde{\rho}_{\min}} \end{aligned} \quad (26)$$

$$\eta_R = \frac{4v_d}{d} h^2 \left[m_{1,2}^{(\text{LB})d}(\tilde{\rho}h^2, u' + 2\tilde{\rho}u'') + m_{1,2}^{(\text{LB})d}(\tilde{\rho}h^2, u') + 2(N_L - 1) m_{1,2}^{(\text{LB})d}(0, u') \right]_{\tilde{\rho}=\tilde{\rho}_{\min}} \quad (27)$$

$$\begin{aligned} \eta_L &= \frac{4v_d}{d} h^2 \left[m_{1,2}^{(\text{RB})d}(\tilde{\rho}h^2, u' + 2\tilde{\rho}u'') + m_{1,2}^{(\text{RB})d}(\tilde{\rho}h^2, u') \right] + \frac{8v_d(d-1)}{d} g^2 \left\{ \right. \\ &\quad \left. \sum_{i=1}^{d_{\text{ad}}} (T_{\hat{n}\hat{n}}^i)^2 \left[m_{1,2}^{(\text{LG})d}(\tilde{\rho}h^2, \mu_{W,i}^2) - m_{1,2}^{(\text{LG})d}(0, \mu_{W,i}^2) - a_3^d(\tilde{\rho}h^2, \mu_{W,i}^2) + a_3^d(0, \mu_{W,i}^2) \right] \right. \\ &\quad \left. + \sum_{a=1}^{N_L} \sum_{i=1}^{d_{\text{ad}}} T_{\hat{n}a}^i T_{a\hat{n}}^i \left[m_{1,2}^{(\text{LG})d}(0, \mu_{W,i}^2) - a_3^d(0, \mu_{W,i}^2) \right] \right\}_{\tilde{\rho}=\tilde{\rho}_{\min}}. \end{aligned} \quad (28)$$

If the direction of the vev \hat{n} has a single nonvanishing component in the chosen basis of fundamental color algebra, i.e. if $\hat{n}^a \propto \delta^{aA}$, the anomalous dimension of the left-handed fermion takes a simpler form

$$\begin{aligned} \eta_L &= \frac{4v_d}{d} h^2 \left[m_{1,2}^{(\text{RB})d}(\tilde{\rho}h^2, u' + 2\tilde{\rho}u'') + m_{1,2}^{(\text{RB})d}(\tilde{\rho}h^2, u') \right] \\ &\quad + \frac{8v_d(d-1)}{d} g^2 \sum_{a=1}^{N_L} \sum_{i=1}^{d_{\text{ad}}} T_{Aa}^i T_{aA}^i \left[m_{1,2}^{(\text{LG})d}(\delta^{aA} \tilde{\rho}h^2, \mu_{W,i}^2) - a_3^d(\delta^{aA} \tilde{\rho}h^2, \mu_{W,i}^2) \right]_{\tilde{\rho}=\tilde{\rho}_{\min}}. \end{aligned} \quad (29)$$

The explicit form of these equations for the linear regulator can be found in App. B.

D. Flow equation for the gauge coupling

Next, we list our results for the flow of the gauge coupling. As only the weak-coupling flow of the gauge cou-

pling is required for the present scenario, we will be satis-

fied essentially with a one-loop approximation. For consistency with the matter sectors, we pay special attention to the threshold behavior, as worked out in greater detail in App. C 1. Since the threshold behavior of the gauge sector depends a bit stronger on the gauge group, we concentrate on the special case $SU(N_L = 2)$ in $d = 4$ Euclidean dimensions. Following Eq. (18), the running gauge coupling can be extracted from the wave function renormalization of the gauge field,

$$\partial_t g^2 = g^2 \eta_W, \quad (30)$$

$$\eta_W = \frac{-g^2}{48\pi^2} \left(22N_L L_W(\mu_{W,i}^2) - d_\gamma N_g L_\psi(\mu_t^2) - L_\phi(\mu_{\phi,a}^2) \right),$$

where the form of the anomalous dimension follows solely from the fact that an additive decomposition into gauge, fermion, and scalar loops can be performed at one-loop order. The threshold functions $L_{W,\psi,\phi}$ parametrize the decoupling of massive modes in the SSB regime. They are normalized by the condition $L_{W,\psi,\phi}(0) = 1$, such that the standard one-loop β function for the gauge coupling is reobtained for massless fluctuations. We also neglect here possible RG improvement from the dependence of these threshold functions on the matter-field anomalous dimensions which contribute at two-loop order.

For $SU(2)$, we use in the present work

$$\begin{aligned} L_W(\mu_W^2) &= \frac{1}{44} \left(21 + \frac{21}{1 + \mu_W^2} + 2 \right), & \mu_W^2 &= \frac{g^2 \kappa}{2}, \\ L_\psi(\mu_t^2) &= \frac{1}{2} \left(1 + \frac{1}{1 + \mu_t^2} \right), & \mu_t^2 &= h^2 \kappa, \\ L_\phi(\mu_H^2) &= \frac{1}{2} \left(1 + \frac{1}{1 + \mu_H^2} \right), & \mu_H^2 &= 2\lambda_2 \kappa, \end{aligned} \quad (31)$$

where we encounter the dimensionless gauge boson, top quark, and Higgs boson masses as defined in Eq. (20).

As detailed in the Appendix, ambiguities can arise for the derivation of the threshold behavior from the choice of the relative orientation between the scalar vev in fundamental color space and the background color field in adjoint color space. These ambiguities correspond to slightly different definitions of the gauge coupling. Furthermore, the computation of the fermionic threshold behavior contains a minor uncertainty which is not resolved in the present work. Nevertheless, all qualitative details of the main asymptotic safety scenario of the present work do not depend on these issues. As a radical check, we have verified the existence of the fixed point also for a pure one-loop form of the gauge β function.

E. Mass parametrization

Before we turn to an analysis of the flow equations, let us discuss the redundancy contained in the list of dimensionless mass and coupling parameters introduced above. For simplicity, we consider the effective potential

only to order ϕ^4 here; generalizations to higher expansion coefficients $\lambda_{\geq 3}$ are straightforward.

A standard viewpoint on the flow equations is the following: as the matter-field anomalous dimensions are defined by purely algebraic equations, cf. Eqs. (26), (27), (28), they can be solved as a function of the dimensionless couplings and the vev $\kappa, \lambda_2, h^2, g^2$ in the SSB regime (analogously in the symmetric regime). Substituting the anomalous dimensions into the flows of these parameters, yields the flow equations for the matter sector,

$$\begin{aligned} \partial_t \kappa &= \beta_\kappa(\kappa, \lambda_2, h^2, g^2), \\ \partial_t \lambda_2 &= \beta_\lambda(\kappa, \lambda_2, h^2, g^2), \\ \partial_t h^2 &= \beta_h(\kappa, \lambda_2, h^2, g^2), \end{aligned}$$

which together with the flow of the gauge coupling Eq. (30) forms a consistent and closed set of flow equations. In this standard parametrization, the dimensionless mass parameters $\mu_{W,t,\phi}$ are considered as composed out of the couplings and the vev κ according to their definitions (19).

It turns out that the alternative viewpoint of formulating the flow in terms of the mass parameters is particularly useful for the present system in the SSB regime. For simplicity, let us discuss this viewpoint for $SU(N_L = 2)$, where the mass parameters are given by $\mu_{W,t,H}$, cf. Eq. (20). In this formulation, we still keep the flow of the gauge coupling Eq. (30) understood as a function of these three mass parameters, cf. Eq. (31). The flow of the mass parameters can then be deduced from Eqs. (32) according to

$$\begin{aligned} \partial_t \mu_H^2 &= 2(\partial_t \kappa) \lambda_2 + 2\kappa(\partial_t \lambda_2), \\ \partial_t \mu_t^2 &= (\partial_t \kappa) h^2 + \kappa(\partial_t h^2), \\ \partial_t \mu_W^2 &= \frac{1}{2}(\partial_t \kappa) g^2 + \frac{1}{2}\kappa(\partial_t g^2), \end{aligned}$$

where κ, h^2, λ_2 in turn are expressed in terms of the mass parameters on the right-hand side.

IV. FIXED POINT STRUCTURE OF THE MODEL

A. Asymptotic safety

For the construction of an asymptotic safety scenario, see [42] for reviews, a fixed-point with suitable UV properties is required. Parametrizing the effective action Γ_k by a possibly infinite set of generalized dimensionless couplings g_i , the Wetterich equation provides us with the corresponding β functions $\partial_t g_i = \beta_{g_i}(g_1, g_2, \dots)$. A fixed point g_i^* satisfies

$$\beta_i(g_1^*, g_2^*, \dots) = 0, \quad \forall i, \quad (32)$$

and is called non-Gaussian, if at least one coupling is non-vanishing $g_j^* \neq 0$. The properties of the fixed point can

be quantified by its critical exponents. Linearizing the flow in the fixed-point regime,

$$\partial_t g_i = B_i^j (g_j - g_j^*) + \dots, \quad B_i^j = \left. \frac{\partial \beta_{g_i}}{\partial g_j} \right|_{g=g^*}, \quad (33)$$

we obtain the critical exponents θ_i as the eigenvalues of the negative Jacobian ($-B_i^j$), which corresponds to the stability matrix. All eigendirections with $\theta_i < 0$ decrease rapidly towards the IR and thus are irrelevant for the long-range physics. All relevant directions with exponents $\theta_i > 0$ grow rapidly towards the IR and thus dominate the long range observables. The marginal directions with $\theta_i = 0$ need to be further classified into marginally-irrelevant and marginally-relevant directions according to their behavior at higher orders in the expansion about the fixed point; e.g. the asymptotically free gauge coupling is marginally relevant. In total, the number of relevant and marginally-relevant directions equals the number of physical parameters to be determined by measurements. An asymptotically safe theory has predictive power, if this number is finite. At the Gaussian fixed point $g_i^* = 0$, this discussion agrees with the standard perturbative power-counting analysis with the critical exponents being identical to the canonical dimensions of the couplings.

A theory allows for an asymptotically safe UV completion, if a non-Gaussian fixed point with a finite number of UV attractive (relevant or marginally-relevant) directions exists. Then, renormalized trajectories emanating from the fixed point can be constructed that correspond to quantum field theories valid to arbitrarily high energy scales.

B. Parameter constraints

As we are working within a truncated theory space, we have to make sure that possible fixed points do not correspond to mere artifacts of our truncation. The following discussion of constraints follows that of [7]. The use of a derivative expansion as our expansion scheme suggests that the quality of the expansion can be deduced from the quantitative influence of higher derivative operators onto the flow of leading-order operators. In our truncation, the leading-order effective potential as well as the Yukawa coupling receive higher-order contributions only through the anomalous dimensions. Therefore, convergence of the derivative expansion requires

$$\eta_L, \eta_R, \eta_\phi \lesssim \mathcal{O}(1). \quad (34)$$

A similar constraint for the gauge-field anomalous dimension η_W is automatically satisfied as long as we consider only weak gauge couplings. Any fixed-point violating Eq. (34) is likely to be an artifact of the present truncation.

Further constraints arise from the form of the effective potential. In the symmetric regime, u should exhibit

a minimum at vanishing field and should be bounded from below. In the polynomial expansion, these criteria translate into

$$m^2, \lambda_{n_{\max}} > 0,$$

where n_{\max} denotes the highest order taken into account in a truncated polynomial expansion of the effective potential. Analogously, the SSB regime requires a positive minimum, $\kappa > 0$, the potential should again be bounded. In addition, the potential at the minimum must have positive curvature implying

$$\kappa, \lambda_{n_{\max}}, \lambda_2 > 0.$$

Hermiticity of the Minkowskian action or Osterwalder-Schrader positivity of the Euclidean action requires

$$h^2 > 0, \quad g^2 > 0,$$

which physically is related to Dyson's vacuum stability argument.

In the mass parametrization for the SSB regime, the above constraints automatically imply that all mass parameters are non-negative, $\mu_{W,t,\phi}^2 \geq 0$. From within the mass parametrization, an independent though somewhat weaker argument can be derived from the general convexity property of the flow equation [43]. For the linear regulator used in this work, convexity implies that $\mu_{W,t,\phi}^2 > -1$ which physically implies that the regularized propagators have a finite gap.

C. Non-Gaussian matter fixed point at finite gauge coupling

Here and in the following, we exclusively concentrate on $SU(N_L = 2)$. For illustrative purposes, we will mainly consider the simplest case of one fermion generation $N_g = 1$. Though this model in isolation would have a global Witten anomaly, cf. footnote 1, it is phenomenologically more reminiscent to the top-Higgs sector of the standard model. In App. D, we verify explicitly that the properties of the anomaly-free $N_g = 2$ model are essentially identical to the results discussed in the following. In order to get an intuition for the flow equations, we start with the standard formulation in terms of the couplings and the effective potential. The case of exactly vanishing gauge coupling was investigated intensively in [7]. In fact, the only possible fixed point is the Gaussian gauge fixed point at $g^2 = 0$ in the weak gauge-coupling regime. However, as this fixed point is only approached asymptotically, let us first search for possible non-Gaussian fixed point structures in the matter sector, keeping the gauge coupling fixed at a given value. For simplicity, we truncate the effective potential at ϕ^4 level.

In fact, for a given finite value of g^2 , the matter system shows a non-Gaussian fixed point in the SSB regime. Note that this fixed point is different from the one found

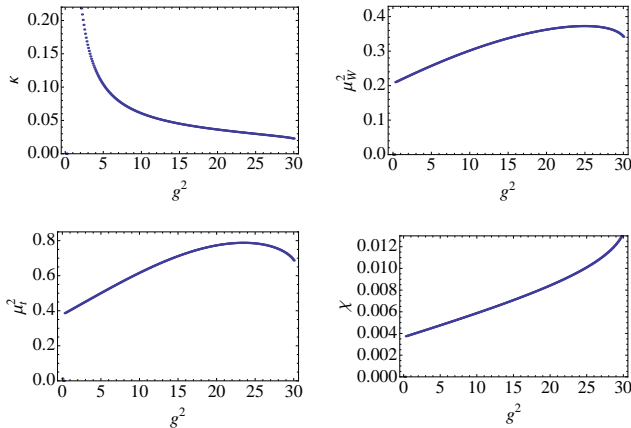


FIG. 1: Non-Gaussian matter fixed points for $N_L = 2$ as a function of an artificially fixed gauge coupling. Whereas the vev κ diverges for $g^2 \rightarrow 0$, the matter couplings approach zero in such a way that the dimensionless mass parameters μ_W^2 and μ_t^2 and the ratio $\chi = \mu_H^2/g^2$ tend to finite values, parametrizing a true fixed point \mathcal{A} of the full system.

at the leading-order of the derivative expansion in [7]. Most importantly, the present fixed point is not destabilized at next-to-leading order in the derivative expansion. As an interesting feature, we observe a strong dependence of the fixed point values on the gauge coupling. In particular, the position of the minimum κ diverges with $g^2 \rightarrow 0$, whereas the Yukawa coupling as well as the scalar self-interaction approach zero in the same limit. We observe that the dimensionless gauge and top mass parameters μ_W^2, μ_t^2 approach finite fixed point values for $g^2 \rightarrow 0$, whereas the dimensionless Higgs mass parameter μ_H^2 vanishes. The latter feature implies that the effective fixed-point potential becomes exceedingly flat for $g^2 \rightarrow 0$. The ratio $\chi = \mu_H^2/g^2$ approaches a finite constant in this limit, implying that λ_2 decreases $\sim g^4$ at the fixed point. These results are depicted in Fig.1. The fixed point associated with the limit $g^2 \rightarrow 0$ will be called \mathcal{A} in the following.

At first sight, this fixed point in the limit $g^2 \rightarrow 0$ seems to be identical to the Gaussian fixed point, as all couplings vanish and only massive free particles remain. This conclusion is, however, wrong for a number of reasons: first, the true Gaussian fixed point of the present model has massless gauge bosons and massless chiral fermions and massless or massive scalar excitations satisfying $U(N_L)$ symmetry. Second, the dimensionless mass parameters observed above arise from a subtle interplay of the interaction terms in the flow equations in the weak-coupling limit; they are a genuine interaction effect. Third, a massive Gaussian fixed point would not only violate the symmetries, but also permit any value for the dimensionful masses which would correspond to fixed scales. In our case, the dimensionless mass parameters approach fixed points and thus do not define any scale. Fourth, the crit-

ical exponents of this fixed point, computed below, do not agree with the canonical dimensions at the Gaussian fixed points.

So far, we have determined the fixed points of the pure matter system for a given finite gauge coupling. Strictly speaking, the curves shown in Fig. 1 do not correspond to fixed points except for the points at $g^2 \rightarrow 0$, where also the gauge coupling has a fixed point. In order to analyze this fixed point more properly, we now turn to the mass parametrization introduced in Sect. III E.

D. Non-Gaussian fixed points in the mass parametrization

Let us analyze the fixed-point structure on the basis of the matter flow equations in mass parametrization Eqs. (32) read together with the gauge coupling flow. From the preceding analysis, we already infer that the ratio

$$\chi = \frac{\mu_H^2}{g^2}, \quad (35)$$

approaches a constant at the desired fixed point. Hence, we consider the right-hand sides of these flow equations in the limit $g^2 \rightarrow 0$ for finite μ_t^2, μ_W^2, χ . In this limit, the fixed point conditions

$$\partial_t g^2 = 0, \quad \partial_t \mu_H = 0, \quad (36)$$

are automatically satisfied. Nontrivial information remains encoded in the flow of the new variable χ ,

$$\partial_t \chi^2 = \frac{1}{g^2} \partial_t \mu_H^2 - \frac{\mu_H^2}{g^4} \partial_t g^2, \quad (37)$$

the $g^2 \rightarrow 0$ limit of which remains finite on the right-hand side except for the fixed points computed below.

As a particular property, we observe that the flows of μ_t^2, μ_W^2 become degenerate,

$$\partial_t \mu_t^2 = \frac{\mu_t^2}{\mu_W^2} (\partial_t \mu_W^2). \quad (38)$$

This degeneracy has an important consequence: possible fixed points for the remaining matter sector parametrized in terms of the three variables (χ, μ_t^2, μ_W^2) have to be determined from only two independent equations, Eqs. (37), and (38). This implies that for any non-trivial fixed point a degenerate one-parameter family, i.e., a line of fixed points has to exist. Since the degeneracy encoded in Eq. (38) becomes exact only in the limit $g^2 \rightarrow 0$ (together with $\mu_H^2 \rightarrow 0$ and μ_W^2, μ_t^2, χ finite), this line of fixed points remains invisible in the standard parametrization by approaching the fixed point $g_*^2 = 0$ from finite values of g^2 .

Knowing already from the preceding standard analysis that a fixed point exists, let us now search for the corresponding line of fixed points within the mass

parametrization, by looking for fixed point solutions satisfying $\partial_t \chi = 0$ and $\partial_t \mu_t^2 = 0$. The reduced flow equation for the top mass parameter in the above mentioned limit reads

$$\partial_t \mu_t^2 = -2\mu_t^2 + \frac{\mu_t^2}{8\pi^2 \chi} \left(\frac{9}{4(1 + \mu_W^2)^2} - \frac{\mu_t^2}{\mu_W^2(1 + \mu_t^2)^2} \right). \quad (39)$$

The correspondingly reduced fixed point equation $\partial_t \chi = 0$ yields exactly one solution, reading

$$\chi^* = -\frac{1}{16\pi^2} \left(\frac{\mu_t^2(1 + 3\mu_t^2)}{(1 + \mu_t^2)^3 \mu_W^2} - \frac{9(1 + 3\mu_W^2)}{4(1 + \mu_W^2)^3} \right). \quad (40)$$

We can plug this result into the flow equation (39) for μ_t^2 to solve for fixed points, giving three solutions for μ_W^2 as a function of μ_t^2 . The solutions with positive, real masses μ_t^2 and μ_W^2 are depicted in Fig.2. Apart from our main solution (solid line), the second solution (dashed lines) results in negative values for χ^* and hence also for μ_H^2 , and therefore will be discarded in the remainder. As the flows of μ_t^2 and μ_W are proportional, their ratio remains undetermined and thus parametrizes a line of fixed points as expected above.

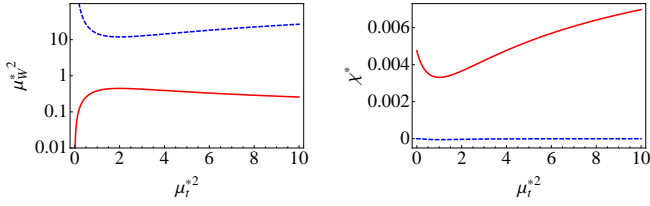


FIG. 2: Fixed point values for μ_W^2 (left panel) and χ (right panel) as a function of the fixed point value of μ_t^2 for $N_L = 2$. Our main solution is shown as a solid line, whereas the dashed line depicts a second solution with legitimate values of the gauge and fermion sector, but a (physically inadmissible) negative χ .

It is reassuring to observe that the fixed point \mathcal{A} identified in the standard parametrization of the flow equations in Subsect. IV C in the limit $g^2 \rightarrow 0$,

$$\mathcal{A} : (\mu_t^{*2}, \mu_W^{*2}, \chi^*) \simeq (0.38, 0.21, 0.0037), \quad (41)$$

cf. Fig.1, is exactly on the (physically admissible) line of fixed points. Along this line, we observe that for $\mu_t^{*2} = \mathcal{O}(1)$, we have $\mu_W^{*2} \simeq \mathcal{O}(0.1, \dots, 1)$, but a much smaller $\chi^* = \mathcal{O}(10^{-3})$. These properties also affect the typical mass hierarchy in the IR, see below.

Let us finally compute the critical exponents θ_i along the line of fixed points from the stability matrix, as defined in Eq. (33), in terms of the generalized couplings g_j within the mass parametrization $\{g^2, \mu_t^2, \mu_W^2, \chi\}$. The results for the critical exponents are depicted in Fig. 3 as a function of the fixed point value μ_t^{*2} . Two of the four critical exponents are zero. Two others start off at

$\theta_1 = 2$, $\theta_2 = 0$, respectively, for $\mu_t^{*2} = 0$, i.e., at the same values as the canonical dimensions at the Gaussian fixed point, but then approach each other for finite μ_t^{*2} , merging at $\mu_t^{*2} \simeq 0.35$. For $\mu_t^{*2} > 0.35$ they form a complex pair with equal real part, $\text{Re}\theta_{1,2} = 1$ and conjugate imaginary parts, as shown in the right panel of Fig. 3.

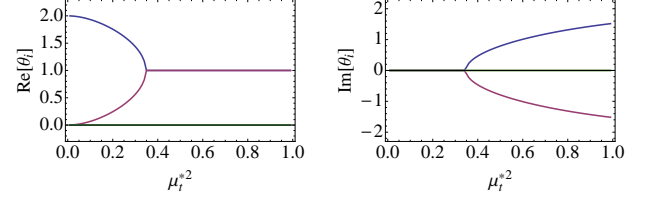


FIG. 3: Critical exponents for the line of fixed points computed in the mass parametrization as a function of the fixed point top mass parameter μ_t^{*2} for $N_L = 2$; left panel: real parts, right panel: imaginary parts. The fixed point near $\mu_t^{*2} \simeq 0.35$, where the two positive exponents merge and start to form a complex pair, corresponds to the fixed point \mathcal{B} introduced below.

As a particular example, let us list the critical exponents at the fixed point \mathcal{A} already discovered in the standard parametrization of the flow given in Eq. (41). These exponents are given by

$$\mathcal{A} : \theta_{1/2} = 1 \pm 0.36i, \theta_3 = \theta_4 = 0. \quad (42)$$

The first two critical exponents form a complex pair and thus describe a spiraling approach towards the fixed point on the corresponding UV critical hypersurface. One of the marginal directions points along the direction of the gauge coupling. From asymptotic freedom of the gauge sector, we can infer that this is a marginally-relevant direction. The other marginal direction is related to the existence of a line of fixed points. This direction must be exactly marginal in our truncation, as a perturbation of the couplings at a given fixed point along the line of fixed points just puts the system onto another fixed point where the flow vanishes completely.

Another special example is the fixed point \mathcal{B} : $(\mu_t^{*2}, \mu_W^{*2}, \chi^*) \simeq (0.35, 0.19, 0.0037)$, denoting the branch point where the two largest real exponents start to form a complex pair. Exactly at \mathcal{B} , we have $\theta_{1/2} = 1$, $\theta_{3,4} = 0$.

To summarize, we have identified a line of UV stable fixed points that can serve to define UV complete quantum field theories of gauged Higgs-Yukawa models by means of suitable RG trajectories that emanate from the fixed point in the UV. Specifying a certain trajectory yields a fully predictive long-range theory. It is instructive to compare our asymptotically safe models with the standard Gaussian fixed point used for perturbative renormalization; theories near the Gaussian fixed points have to be defined in terms of four physical parameters corresponding, for instance, to the relevant mass parameter of the Higgs potential, and the marginal scalar self-interaction, Yukawa coupling and gauge coupling.

By contrast, in the present asymptotically safe model defined in terms of a trajectory emanating from a fixed point, each trajectory is defined in terms of three physical parameters corresponding to the two relevant directions and the marginally relevant gauge coupling. The fourth parameter does not correspond to a physical parameter in a particular theory, but corresponds to choosing one fixed point on the line of fixed points, i.e., choosing among a one-parameter family of theories. Of course, this difference in the conceptual meaning of parameters is not substantial from a pragmatic viewpoint, as in total four different measurements are needed in order to fix the long-range behavior of the system unambiguously.

Whether or not the existence of a line of fixed points also holds beyond our truncation cannot be told from the present investigation. It is at least well conceivable that the degeneracy manifested by Eq. (38) is lifted by the influence of higher order operators. If so, only a finite number of fixed points might remain, thus potentially also reducing the number of physical parameters as observed in the ungauged Yukawa models [6, 7].

V. FLOW FROM THE ULTRAVIOLET TO THE ELECTROWEAK SCALE

For the asymptotically safe models discovered above to be viable building blocks of the standard model Higgs sector, we need to show that the UV critical hypersurface contains trajectories that end up in the Higgs phase of the model with massive gauge bosons, a massive top quark and a massive scalar Higgs boson. This is indeed the case as we demonstrate in the following by integrating the RG flow for different sets of initial conditions towards the long-range physics.

Since the fixed points exhibit positive critical exponents of order $\mathcal{O}(1)$, we face the standard technical problem that initial conditions near the fixed points have to be fine-tuned in order to separate the UV scale from the scale of IR observables. The necessary fine-tuning in the Yukawa sector is complicated by the marginally-relevant gauge sector which has to be UV adjusted as to provide for a suitable IR coupling strength. This suitable UV adjustment is not a conceptual problem, but merely a tedious search for the desired initial conditions which can straightforwardly be solved, e.g., by suitable bisection techniques. In the present case, this problem is slightly complicated by the fact that the line of fixed points only becomes visible in the limit $g^2 \rightarrow 0$. In order to ensure that the flow is started sufficiently near the line of fixed points, we thus have to start in the deep UV where g^2 is sufficiently small.

For simplicity, we will choose such a small value in the following flow examples. We set $g^2 = 1/2000$ at an arbitrary initialization scale $t_{\text{init}} = \ln k/\Lambda = 10$. In the present work, this scale has a meaning of an intermediate scale, separating the infrared $t < 10$, where the IR observables and the mass spectrum are built up, from

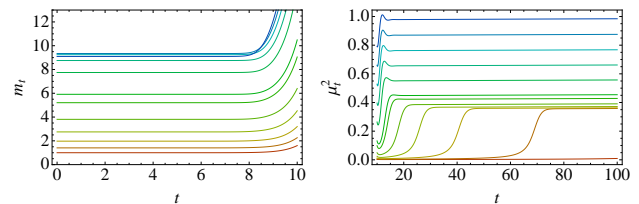


FIG. 4: Right plot: typical UV flows to the line of fixed points for the dimensionless parameter μ_t^2 . Left plot: corresponding IR trajectories for the dimensionful top mass with freeze-out. The set of curves corresponds to different values of μ_t^2 at the intermediate scale $t = 10$ (larger to smaller from top to bottom) and are normalized such that the smallest initial μ_t^2 value yields a top mass $m_t = 1$ in arbitrary units.

the flow towards the fixed point regime for $t > 10$. Typical flows ending up in the Higgs phase are shown in Fig. 4. All these flows are initiated near the line of UV fixed points starting with different values of μ_t^2 within the interval $[10^{-5}, 0.8]$ at $t_{\text{init}} = 10$. For the remaining two variables, μ_W^2 and χ , we employ initial values that lie close to the fixed point corresponding to the current choice of μ_t^2 , cf. Fig. 2. In the deep UV (right panel), the flows approach the line of fixed points at different values of μ_t^{*2} (and corresponding values of μ_W^{*2} and χ^*). Towards the IR, the flows rapidly freeze out, implying that the dimensionful mass parameters such as m_t approach finite values (left panel). The units are arbitrary and chosen such that the lowest trajectory yields an IR value of 1 for the top mass m_t . We observe a very similar behavior for the other two mass variables, with the dimensionless parameters μ_W^2 and χ approaching their corresponding fixed points in the UV and the dimensionful counterparts m_W and m_H freezing out at finite values in the IR. The gauge coupling exhibits the perturbative asymptotically free log-running including the slight threshold modifications in the UV, whereas the log-running is more strongly modified in the IR because of the decoupling of massive modes.

These flows illustrate our conclusion that the UV line of fixed points render the present gauged Higgs-Yukawa model asymptotically safe. Whereas the IR exhibits a standard Higgs phase indistinguishable from the perturbative standard scenario, the UV is controlled by a fixed point at which the continuum limit can be taken. The theory thus is UV complete.

In addition to these results which can already be anticipated from the pure fixed point analysis, we observe further aspects of our model which require the solutions of the flow equation: for flows starting at generic values of μ_t^2, μ_W^2, χ near the line of fixed points, the hierarchy of the fixed point values is transmuted into a similar hierarchy of the particle masses: e.g., for typical flows that approach a fixed point with μ_t^2 of order $\mathcal{O}(0.1, \dots, 1)$, we read off from Fig. 2 (right panel), that the corresponding χ values are typically two orders of magnitude smaller,

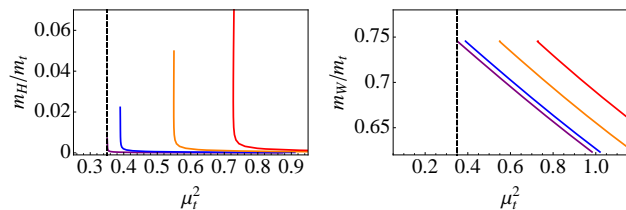


FIG. 5: Compilation of IR results for flows starting on the line of fixed points, as a function of the dimensionless mass parameter μ_t^2 in the deep UV for four different starting values of the gauge coupling $g^2 \in \{10^{-4}, 5 \cdot 10^{-5}, 10^{-5}, 10^{-6}\}$ (red, orange, blue and purple, respectively) at $t = 10$. The deep UV value of μ_t^2 is read off at a rather extreme reference scale $t = 30000$. Whereas the W to top mass ratio remains within a very narrow range by choosing natural initial conditions (right panel), realistic Higgs-to-top mass ratios can be approached for specifically tuned flows (left panel). In the limit of weak gauge coupling, these tuned flows appear to be connected with the branching fixed point \mathcal{B} (dashed lines).

whereas μ_W^2 is also of order μ_t^2 in this regime (left panel). The same hierarchy then generically remains present in the mass spectrum: the top and W mass are of the same order, whereas the Higgs mass is typically about two orders of magnitude smaller.

This preservation of UV-IR hierarchy is lifted, if the system is tuned to certain values which depend a bit on the value of the gauge coupling at the initialization scale t_{init} . For these specifically tuned flows, the UV behavior still exhibits the parameter hierarchy, whereas the IR can behave differently. A variety of UV-IR solutions for varying initial condition μ_t^2 at t_{init} are compiled in Fig. 5 and depicted as a function of the deep UV value for μ_t^2 (read off at $t > 130$, cf. Fig. 4). These initial conditions have been chosen such that the W mass to top mass ratio remains slightly above the physical value near $\simeq 0.5$, as shown in the right panel. This implies that, as the top mass increases by a factor of two, also the W mass is about twice as large. This is different for the Higgs mass (left panel), which generically is two orders of magnitude smaller than the top mass. Only for the particularly tuned trajectories, the situation changes and we find Higgs mass to top mass ratios ultimately approaching the realistic ratio $125/175 \simeq 0.7$. Four such trajectory sets with corresponding tuning are shown in Fig. 5 for different values of the gauge coupling $g^2 \in \{10^{-4}, 5 \cdot 10^{-5}, 10^{-5}, 10^{-6}\}$ at t_{init} .

The particularities of these specifically tuned flows become obvious from the behavior of the trajectories at intermediate scales. Whereas generic flows consist of a UV fixed-point regime, an IR freeze-out regime and a cross-over in between, flows that lead to larger Higgs masses exhibit an additional quasi-fixed-point regime at intermediate scales. This “walking” behavior is, for instance, visible for the lower lines in Fig. 4 (right panel), showing a cross-over from the UV fixed point to an intermedi-

ate walking regime which can extend over a wide range of scales. This intermediate regime is characterized by small values of the dimensionless mass parameters. The corresponding β functions are obviously small here but non-vanishing. We interpret this walking regime as the remnant of the line of the ($g^2 \rightarrow 0$) fixed points at finite values of g^2 .

It is interesting to observe that trajectories exhibiting this walking regime are connected with sharply defined fixed point values of μ_t^{*2} . The latter in turn depends on the initial choice for the value of the gauge coupling. In the limit of small initial gauge coupling, our results indicate that the trajectories approach the branching fixed point \mathcal{B} with $\mu_t^{*2} \simeq 0.35$, cf. dashed lines in Fig. 5. In our parameter scans, we have not been able to find trajectories that emanate from the line of fixed points at values $\mu_t^{*2} < 0.35$. This might indicate that the RG flow close to this branch of the line of fixed points is rather strong. This would go along with the fact that the value of the largest critical exponent increases for smaller μ_t^{*2} , cf. Fig. 3 (left panel), such that finding those trajectories requires more sophisticated fine-tuning procedures. Alternatively, these fixed points might not be directly connected to a massive Higgs phase in the IR. These questions deserve further study.

VI. CONCLUSIONS

We have discovered a line of interacting fixed points in the RG flow of gauged chiral Higgs-Yukawa models. Each fixed point gives rise to a novel universality class of UV complete asymptotically safe quantum field theories with interacting fermions, gauge fields and elementary scalars. We have demonstrated that UV complete RG trajectories emanating from the line of fixed points exhibit a Higgs phase with massive top quark, gauge bosons and Higgs boson. If similar properties hold for the standard model, the existence of such a line of fixed points solves the triviality problem of the top-Higgs sector of the standard model.

The non-trivial UV behavior is characterized by asymptotic freedom in all interaction couplings and a quasi-conformal behavior in all mass-like parameters. In other words, the fixed point theories live in the symmetry-broken regime with all masses running proportional to the RG scale. In particular, the scalar effective potential approaches asymptotic flatness in the UV, with a non-vanishing minimum increasing inversely proportional to the asymptotically free gauge coupling.

Our computations are based on a functional RG approach at next-to-leading order in a derivative expansion. Our results for the UV behavior at leading order and next-to-leading order are identical, providing evidence for a good convergence of our nonperturbative approximation scheme. In this scheme, we have determined the critical exponents along the line of fixed points, two of which belong to RG relevant directions. The gauge cou-

pling remains a marginally-relevant direction, whereas perturbations along the line of fixed points are exactly marginal. As a consequence, these asymptotically safe theories have one parameter less than their corresponding (non UV-complete) perturbative counterparts near the Gaussian fixed point. However, this one parameter is transmuted into the one-parameter family of fixed points distinguishing different universality classes along the line of fixed points.

We have performed non-exhaustive scans of typical long-range properties of the system in the Higgs phase. A generic feature appears to be that the mass of the Higgs boson is about two orders of magnitude smaller than the top quark mass and the gauge boson mass; the latter masses are typically of similar size. This mass hierarchy is a consequence of a corresponding hierarchy of fixed point values. We observe that this hierarchy can be lifted along special trajectories which exhibit an intermediate walking regime. If similar properties are also found for the full standard model, a construction of a realistic model with improved UV behavior seems within reach.

In this respect, the IR results of the present model are remarkable, since the ‘‘IR window’’, i.e., the physical parameter space accessible in the IR, appears to be rather different from that of the standard model in a perturbative treatment. The latter as well as many of its extensions typically feature upper and lower bounds on the mass of the Higgs boson as a function of the UV cutoff [44] with the recently measured Higgs boson mass [45] being near or even somewhat below the lower bound. The present model therefore provides for an example that a modified nonperturbative UV running of the couplings can strongly influence the shape of the IR window without modifying the particle content or the interactions.

Acknowledgments

We thank Lukas Janssen, Axel Maas, Jan Pawłowski, René Sondenheimer, Gian Paolo Vacca for interesting and enlightening discussions. HG, MMS, and LZ acknowledge support by the DFG under grants GRK1523, Gi 328/5-2 (Heisenberg program) and FOR723. MMS is supported by the grant ERC- AdG-290623. The work of SR is supported by the DFG within the Emmy-Noether program (Grant SA/1975 1-1).

Appendix A: Regulators and threshold functions

1. Regulators

We have to evaluate the r.h.s of eq. (5), for which we need the $\Gamma_k^{(2)}$ matrix. Let us consider the fields ϕ_i , ψ_L , ψ_R , W , c , \bar{c} as column vectors, with a number of components respectively given by N_L , $d_\gamma N_g N_L$, $d_{\bar{\gamma}} N_g$, dd_{ad} , d_{ad} , d_{ad} . Accordingly let us consider ψ_L and ψ_R as row vectors. Taking care of the partly Grassmann-valued field

components and of the Fourier conventions, let us denote by $\Phi^T(q)$ the row vector with components $\phi_1^T(q)$, $\phi_2^T(q)$, $\psi_L^T(q)$, $\psi_R^T(-q)$, $\psi_R^T(q)$, $\bar{\psi}_R(-q)$, $W^T(q)$, $c^T(q)$, $\bar{c}^T(q)$, and by $\Phi(p)$ the column vector given by its transposition. Then $\Gamma_k^{(2)}$ is computed as follows

$$\Gamma_k^{(2)} = \frac{\overrightarrow{\delta}}{\delta\Phi^T(-p)} \Gamma_k \frac{\overleftarrow{\delta}}{\delta\Phi(q)}.$$

For a proper IR regularization, a regulator which is diagonal in field space is sufficient and convenient,

$$R_k(q, p) = \delta(p - q) \begin{pmatrix} R_B & 0 & 0 & 0 & 0 \\ 0 & R_L & 0 & 0 & 0 \\ 0 & 0 & R_R & 0 & 0 \\ 0 & 0 & 0 & R_G & 0 \\ 0 & 0 & 0 & 0 & R_{\text{gh}} \end{pmatrix} (p),$$

with a $2N_L \times 2N_L$ matrix for the scalar bosonic sector

$$R_B(p) = \begin{pmatrix} \delta^{ab} & 0 \\ 0 & \delta^{ab} \end{pmatrix} Z_\phi p^2 r_B(p^2),$$

an $2d_\gamma N_g N_L \times 2d_\gamma N_g N_L$ matrix for the left-handed spinor

$$R_L(p) = - \begin{pmatrix} 0 & \delta^{ab} \not{p}^T \\ \delta^{ab} \not{p} & 0 \end{pmatrix} Z_L r_L(p^2),$$

an $2d_\gamma N_g \times 2d_\gamma N_g$ matrix for the right-handed spinor

$$R_R(p) = - \begin{pmatrix} 0 & \not{p}^T \\ \not{p} & 0 \end{pmatrix} Z_R r_R(p^2),$$

a $dd_{\text{ad}} \times dd_{\text{ad}}$ matrix for the gauge vector boson

$$R_G(p) = Z_W p^2 r_{\text{GT}}(p^2) \Pi_T^{\mu\nu}(p) \delta^{ij} + \frac{Z_\phi p^2 r_{\text{GL}}(p^2)}{\alpha} \Pi_L^{\mu\nu}(p) \delta^{ij},$$

where the Π 's are the usual longitudinal and transverse projectors with respect to p_μ , and a $2d_{\text{ad}} \times 2d_{\text{ad}}$ matrix for the ghosts

$$R_{\text{gh}} = \begin{pmatrix} 0 & \delta^{ij} \\ -\delta^{ij} & 0 \end{pmatrix} p^2 r_{\text{gh}}(p^2).$$

Notice that here and in the whole paper we set $Z_{\text{gh}} = 1$ at any scale, that is: we neglect η_{gh} . Choosing different regulators for the scalar bosons (B), for the transverse gauge bosons (GT), for the longitudinal gauge boson (GL), for the ghosts (gh) and for the left-handed (L) as well as for the right-handed (R) spinors, allows one to write the flow equation in the form

$$\partial_t \Gamma_k = \frac{1}{2} \tilde{\partial}_t \text{STr} \log(\Gamma_k^{(2)} + R_k),$$

where

$$\begin{aligned} \tilde{\partial}_t \equiv & \frac{\partial_t(Z_\phi r_B)}{Z_\phi} \cdot \frac{\delta}{\delta r_B} + \frac{\partial_t(Z_L r_L)}{Z_L} \cdot \frac{\delta}{\delta r_L} \\ & + \frac{\partial_t(Z_R r_R)}{Z_R} \cdot \frac{\delta}{\delta r_R} + \frac{\partial_t(Z_W r_{\text{GT}})}{Z_W} \cdot \frac{\delta}{\delta r_{\text{GT}}} \\ & + \frac{\partial_t(Z_\phi r_{\text{GL}})}{Z_\phi} \cdot \frac{\delta}{\delta r_{\text{GL}}} + \partial_t r_{\text{gh}} \cdot \frac{\delta}{\delta r_{\text{gh}}} \end{aligned} \quad (\text{A1})$$

and \cdot denotes multiplication as well as integration over the common argument of the shape functions of the two factors. After having performed this differentiation we are free to specify the form of the shape functions r . See App. A 2 for an example of such a choice.

2. Threshold functions

Since in the SSB regime one of the left-handed Weyl fermions together with the right-handed one gets massive, it is useful to introduce a superscript (F) to denote the corresponding Dirac fermion. Then the regularized kinetic (or squared kinetic) terms are given by

$$\begin{aligned} P_{\text{B/GT/GL/gh}}(x) &= x(1 + r_{\text{B/GT/GL/gh}}(x)) \\ P_{\text{L}}(x) &= x(1 + r_{\text{L}}(x))^2 \\ P_{\text{F}}(x) &= x(1 + r_{\text{L}}(x))(1 + r_{\text{R}}(x)). \end{aligned}$$

Accordingly, the loop momentum integrals appearing on the r.h.s. of the flow equation are classified, implicitly defining the corresponding threshold functions. In the following, the operator $\tilde{\partial}_t$ is the one defined in Eq. (A1). We also use the abbreviations $\int_p \equiv \int \frac{d^d p}{(2\pi)^d}$ and $v_d = 1/(2^{d+1}\pi^{d/2}\Gamma(d/2))$, such that $v_4 = 1/(32\pi^2)$. Then, the threshold functions read

$$\begin{aligned} l_0^{(\text{B/F/L/gh})d}(\omega) &= \frac{k^{-d}}{4v_d} \int_p \tilde{\partial}_t \log(P_{\text{B/F/L/gh}} + \omega k^2) \\ l_{0\text{T/L}}^{(\text{G})d}(\omega) &= \frac{k^{-d}}{4v_d} \int_p \tilde{\partial}_t \log(P_{\text{GT/GL}} + \omega k^2) \\ l_{n_1, n_2}^{(\text{FB})d}(\omega_1, \omega_2) &= -\frac{k^{2(n_1+n_2)-d}}{4v_d} \\ &\quad \times \int_p \tilde{\partial}_t \frac{1}{(P_{\text{F}} + \omega_1 k^2)^{n_1} (P_{\text{B}} + \omega_2 k^2)^{n_2}} \\ l_{n_1, n_2}^{(\text{BG})d}(\omega_1, \omega_2) &= -\frac{k^{2(n_1+n_2)-d}}{4v_d} \\ &\quad \times \int_p \tilde{\partial}_t \frac{1}{(P_{\text{B}} + \omega_1 k^2)^{n_1} (P_{\text{GT}} + \omega_2 k^2)^{n_2}} \\ m_2^{(\text{F})d}(\omega) &= -\frac{k^{6-d}}{4v_d} \int_p p^2 \tilde{\partial}_t \left(\frac{\partial}{\partial p^2} \frac{1}{P_{\text{F}} + \omega k^2} \right)^2 \\ m_4^{(\text{F})d}(\omega) &= -\frac{k^{4-d}}{4v_d} \\ &\quad \times \int_p p^4 \tilde{\partial}_t \left(\frac{\partial}{\partial p^2} \frac{1 + r_{\text{L}}}{P_{\text{F}} + \omega k^2} \right) \left(\frac{\partial}{\partial p^2} \frac{1 + r_{\text{R}}}{P_{\text{F}} + \omega k^2} \right) \\ m_2^{(\text{G})d}(\omega) &= -\frac{k^{6-d}}{4v_d} \int_p p^2 \tilde{\partial}_t \left(\frac{\partial}{\partial p^2} \frac{1}{P_{\text{GT}} + \omega k^2} \right)^2 \end{aligned}$$

$$\begin{aligned} m_{2,2}^{(\text{B})d}(\omega_1, \omega_2) &= -\frac{k^{6-d}}{4v_d} \\ &\quad \times \int_p p^2 \tilde{\partial}_t \left(\frac{\frac{\partial}{\partial p^2} P_{\text{B}}}{(P_{\text{B}} + \omega_1 k^2)^2} \frac{\frac{\partial}{\partial p^2} P_{\text{B}}}{(P_{\text{B}} + \omega_2 k^2)^2} \right) \\ m_{1,2}^{(\text{LB})d}(\omega_1, \omega_2) &= -\frac{k^{4-d}}{4v_d} \\ &\quad \times \int_p p^2 \tilde{\partial}_t \left(\frac{1 + r_{\text{R}}}{P_{\text{F}} + \omega_1 k^2} \frac{\frac{\partial}{\partial p^2} P_{\text{B}}}{(P_{\text{B}} + \omega_2 k^2)^2} \right) \\ m_{1,2}^{(\text{RB})d}(\omega_1, \omega_2) &= -\frac{k^{4-d}}{4v_d} \\ &\quad \times \int_p p^2 \tilde{\partial}_t \left(\frac{1 + r_{\text{L}}}{P_{\text{F}} + \omega_1 k^2} \frac{\frac{\partial}{\partial p^2} P_{\text{B}}}{(P_{\text{B}} + \omega_2 k^2)^2} \right) \\ m_{1,2}^{(\text{LG})d}(\omega_1, \omega_2) &= -\frac{k^{4-d}}{4v_d} \\ &\quad \times \int_p p^2 \tilde{\partial}_t \left(\frac{1 + r_{\text{R}}}{P_{\text{F}} + \omega_1 k^2} \frac{\frac{\partial}{\partial p^2} P_{\text{GT}}}{(P_{\text{GT}} + \omega_2 k^2)^2} \right) \end{aligned}$$

$$\begin{aligned} a_1^d(\omega) &= -\frac{k^{6-d}}{16v_d} \int_p \frac{1}{p^2} \tilde{\partial}_t \left(\frac{1}{P_{\text{GT}} + \omega k^2} \right)^2 \\ a_3^d(\omega_1, \omega_2) &= -\frac{k^{4-d}}{4v_d} \int_p \tilde{\partial}_t \left(\frac{1 + r_{\text{R}}}{P_{\text{F}} + \omega_1 k^2} \frac{1}{P_{\text{GT}} + \omega_2 k^2} \right). \end{aligned}$$

For practical computations, we use the linear regulator for the scalar bosons, for the gauge bosons and for the ghosts

$$x r_{\text{B/GT/GL/gh}}(x) = (1-x)\theta(1-x), \quad (\text{A2})$$

where $x = q^2/k^2$. For the spinor fermions the linear regulator corresponds to a shape function $r_{\text{L/R}}$ such that $x(1 + r_{\text{B}}(x)) = x(1 + r_{\text{L/R}}(x))^2$. This regulator satisfies an optimization criterion within our present truncation and is technically advantageous, as we can perform all momentum integrations analytically, obtaining

$$\begin{aligned} l_0^{(\text{B})d}(\omega) &= \frac{2}{d} \frac{1 - \frac{\eta_\phi}{d+2}}{1 + \omega}, \\ l_0^{(\text{F})d}(\omega) &= \frac{2}{d} \frac{1 - \frac{\eta_{\text{L}} + \eta_{\text{R}}}{2(d+1)}}{1 + \omega}, \\ l_0^{(\text{L})d}(\omega) &= \frac{2}{d} \frac{1 - \frac{\eta_{\text{L}}}{d+1}}{1 + \omega}, \\ l_{0\text{T}}^{(\text{G})d}(\omega) &= \frac{2}{d} \frac{1 - \frac{\eta_{\text{W}}}{d+2}}{1 + \omega}, \\ l_{0\text{L}}^{(\text{G})d}(\omega) &= \frac{2}{d} \frac{1 - \frac{\eta_\phi}{d+2}}{1 + \omega}, \\ l_0^{(\text{gh})d}(\omega) &= \frac{2}{d} \frac{1}{1 + \omega}, \end{aligned}$$

$$\begin{aligned}
l_{n_1, n_2}^{(\text{FB})d}(\omega_1, \omega_2) &= \frac{2}{d} \left[n_1 \frac{1 - \frac{\eta_L + \eta_R}{2(d+1)}}{(1 + \omega_1)^{1+n_1} (1 + \omega_2)^{n_2}} \right. \\
&\quad \left. + n_2 \frac{1 - \frac{\eta_\phi}{d+2}}{(1 + \omega_1)^{n_1} (1 + \omega_2)^{1+n_2}} \right], \\
l_{n_1, n_2}^{(\text{BG})d}(\omega_1, \omega_2) &= \frac{2}{d} \left[n_1 \frac{1 - \frac{\eta_\phi}{d+2}}{(1 + \omega_1)^{1+n_1} (1 + \omega_2)^{n_2}} \right. \\
&\quad \left. + n_2 \frac{1 - \frac{\eta_W}{d+2}}{(1 + \omega_1)^{n_1} (1 + \omega_2)^{1+n_2}} \right],
\end{aligned}$$

$$\begin{aligned}
m_2^{(\text{F})d}(\omega) &= \frac{1}{(1 + \omega)^4}, \\
m_4^{(\text{F})d}(\omega) &= \frac{1}{(1 + \omega)^4} + \frac{1 - \frac{1}{2}(\eta_L + \eta_R)}{(d-2)(1 + \omega)^3} \\
&\quad - \left(\frac{1 - \frac{1}{2}(\eta_L + \eta_R)}{2d-4} + \frac{1}{4} \right) \frac{1}{(1 + \omega)^2}, \\
m_2^{(\text{G})d}(\omega) &= \frac{1}{(1 + \omega)^4},
\end{aligned}$$

$$\begin{aligned}
m_{2,2}^{(\text{B})d}(\omega_1, \omega_2) &= \frac{1}{(1 + \omega_1)^2 (1 + \omega_2)^2}, \\
m_{1,2}^{(\text{LB})d}(\omega_1, \omega_2) &= \frac{1 - \frac{\eta_\phi}{d+1}}{(1 + \omega_1)(1 + \omega_2)^2}, \\
m_{1,2}^{(\text{RB})d}(\omega_1, \omega_2) &= \frac{1 - \frac{\eta_\phi}{d+1}}{(1 + \omega_1)(1 + \omega_2)^2}, \\
m_{1,2}^{(\text{LG})d}(\omega_1, \omega_2) &= \frac{1 - \frac{\eta_W}{d+1}}{(1 + \omega_1)(1 + \omega_2)^2},
\end{aligned}$$

$$\begin{aligned}
a_1^d(\omega) &= \frac{1 - \frac{\eta_W}{d}}{d-2} \frac{1}{(1 + \omega)^3}, \\
a_3^d(\omega_1, \omega_2) &= \frac{2}{d-1} \frac{1 - \frac{\eta_W}{d+1}}{(1 + \omega_1)(1 + \omega_2)^2} \\
&\quad + \frac{1}{d-1} \frac{(1 - \frac{\eta_L}{d}) - \omega_1 (1 - \frac{\eta_R}{d})}{(1 + \omega_1)^2 (1 + \omega_2)}.
\end{aligned}$$

Appendix B: Derivation of the flow equations for the matter sector

The computation of the RG flow of the matter sector inside the truncation (9) will be sketched. For further details see [46].

1. Flow equation for the potential

The flow of the potential can be computed by setting the field ϕ^a to a constant value and all the other fields to zero. This projects both sides of the flow onto the scalar potential. Then, in Landau gauge the matrix $\Gamma_k^{(2)} + R_k$ can be inverted easily. Multiplying with the derivative of the regulator, and taking the supertrace yields the result. This can be interpreted as an improved one-loop computation for a 0-point function, i.e. a sum over all the one-loop graphs with no external legs. The gauge contribution takes the form of a closed gauge boson propagator, and since it does not involve any vertex, it should not explicitly depend on \bar{g} . Indeed we get

$$\begin{aligned}
\partial_t U &= \frac{1}{2} \int \frac{d^d p}{(2\pi)^d} \partial_t P_B \left[\frac{2N_L - 1}{Z_\phi P_B + U'} + \frac{1}{Z_\phi P_B + U' + 2\rho U''} \right] \\
&\quad - d_\gamma N_g \int \frac{d^d p}{(2\pi)^d} \left\{ \left[(N_L - 1) + \frac{Z_L Z_R P_F}{Z_L Z_R P_F + \rho \bar{h}^2} \right] \frac{\partial_t [Z_L r_L]}{Z_L (1 + r_L)} + \frac{Z_L Z_R P_F}{Z_L Z_R P_F + \rho \bar{h}^2} \frac{\partial_t [Z_R r_R]}{Z_R (1 + r_R)} \right\} \\
&\quad + \frac{1}{2} \sum_{i=1}^{N_L^2 - 1} \int \frac{d^d p}{(2\pi)^d} \left[(d-1) \frac{\partial_t (Z_W p^2 r_{\text{GT}})}{Z_W P_{\text{GT}} + \bar{m}_{W,i}^2} + \frac{\partial_t (Z_\phi p^2 r_{\text{GL}})}{Z_\phi P_{\text{GL}}} \right] - \int \frac{d^d p}{(2\pi)^d} \frac{d_{\text{ad}} p^2 \partial_t r_{\text{gh}}}{P_{\text{gh}}}
\end{aligned}$$

that is, in terms of threshold functions

$$\begin{aligned}
\partial_t U &= 2v_d k^d \left\{ (2N_L - 1) l_0^{(\text{B})d} \left(\frac{U'}{Z_\phi k^2} \right) + l_0^{(\text{B})d} \left(\frac{U' + 2\rho U''}{Z_\phi k^2} \right) - d_\gamma N_g \left[(N_L - 1) l_0^{(\text{L})d}(0) + 2l_0^{(\text{F})d} \left(\frac{\rho \bar{h}^2}{Z_L Z_R k^2} \right) \right] \right. \\
&\quad \left. - 2d_{\text{ad}} l_0^{(\text{gh})d}(0) + \sum_{i=1}^{d_{\text{ad}}} \left[(d-1) l_{0\text{T}}^{(\text{G})d} \left(\frac{\bar{m}_{W,i}^2}{Z_W k^2} \right) + l_{0\text{L}}^{(\text{G})d}(0) \right] \right\}
\end{aligned}$$

where U is a function of ρ . Switching to dimensionless quantities this becomes Eq. (23).

2. Flow equation for the Yukawa coupling

For the derivation of the flow of the Yukawa coupling, we first separate the bosonic field into the vev and a

purely radial deviation from the vev. This corresponds

to setting $\Delta\phi_2 = 0$ in Eq. (6). While this is irrelevant in the symmetric regime, it makes a difference in the SSB regime, as it projects onto the Yukawa coupling between the fermions and Higgs boson, being the radial mode. The projection of the flow equation onto such an operator reads

$$\partial_t \bar{h} = - \frac{1}{\sqrt{2}} \frac{\overrightarrow{\delta}}{\delta \bar{\psi}_L^{\hat{n}}(p)} \frac{\overrightarrow{\delta}}{\delta \Delta \phi_1^{\hat{n}}(p')} \partial_t \Gamma_k \frac{\overleftarrow{\delta}}{\delta \psi_R(q)} \Big|_0. \quad (\text{B1})$$

The vertical line indicates that the equation is evaluated at vanishing momenta $p' = p = q = 0$ and at vanishing fluctuation fields. Next, we can decompose the matrix $(\Gamma_k^{(2)} + R_k)$ into two parts. One part, which we call $(\Gamma_{k,0}^{(2)} + R_k)$, contains only v and is independent of the fluctuations. The remaining part, $\Delta\Gamma_k^{(2)}$, contains all fluctuating fields. Using the $\tilde{\partial}_t$ -notation of App. A 2 and expanding by means of the Mercator series, the flow equation can be written as

$$\begin{aligned} \partial_t \Gamma_k &= \frac{1}{2} \sum_{s=1}^{\infty} \frac{(-)^{s+1}}{s} \text{STr} \tilde{\partial}_t \left[\left(\frac{\Delta\Gamma_k^{(2)}}{\Gamma_{k,0}^{(2)} + R_k} \right)^s \right] \\ &+ \frac{1}{2} \text{STr} \tilde{\partial}_t \log(\Gamma_{k,0}^{(2)} + R_k). \end{aligned} \quad (\text{B2})$$

$$\begin{aligned} \partial_t \bar{h} &= - \frac{\bar{h}^3}{2} \int \frac{d^d p}{(2\pi)^d} \tilde{\partial}_t \left[\frac{1}{Z_L Z_R P_F + \rho \bar{h}^2} \left(\frac{2\rho U''}{(Z_\phi P_B + U')^2} - \frac{6\rho U'' + 4\rho^2 U'''}{(Z_\phi P_B + U' + 2\rho U'')^2} \right) \right. \\ &+ \frac{2\rho \bar{h}^2}{(Z_L Z_R P_F + \rho \bar{h}^2)^2} \left(\frac{1}{Z_\phi P_B + U'} - \frac{1}{Z_\phi P_B + U' + 2\rho U''} \right) \\ &\left. - \frac{1}{Z_L Z_R P_F + \rho \bar{h}^2} \left(\frac{1}{Z_\phi P_B + U'} - \frac{1}{Z_\phi P_B + U' + 2\rho U''} \right) \right] \end{aligned}$$

where the whole r.h.s. should be evaluated at the value $\rho = \frac{1}{2} \bar{v}^2$ that minimizes the potential U . In terms of the threshold functions as defined in App. A 2 this reads

$$\begin{aligned} \partial_t \bar{h}^2 &= \frac{4v_d \bar{h}^4}{Z_L Z_R Z_\phi k^{4-d}} \left[\frac{2\rho U''}{Z_\phi k^2} l_{1,2}^{(\text{FB})d} \left(\frac{\rho \bar{h}^2}{Z_L Z_R k^2}, \frac{U'}{Z_\phi k^2} \right) - \frac{6\rho U'' + 4\rho U'''}{Z_\phi k^2} l_{1,2}^{(\text{FB})d} \left(\frac{\rho \bar{h}^2}{Z_L Z_R k^2}, \frac{U' + 2\rho U''}{Z_\phi k^2} \right) \right. \\ &+ \frac{2\rho \bar{h}^2}{k^2} l_{2,1}^{(\text{FB})d} \left(\frac{\rho \bar{h}^2}{Z_L Z_R k^2}, \frac{U'}{Z_\phi k^2} \right) - \frac{2\rho \bar{h}^2}{k^2} l_{2,1}^{(\text{FB})d} \left(\frac{\rho \bar{h}^2}{Z_L Z_R k^2}, \frac{U' + 2\rho U''}{Z_\phi k^2} \right) \\ &\left. - l_{1,1}^{(\text{FB})d} \left(\frac{\rho \bar{h}^2}{Z_L Z_R k^2}, \frac{U'}{Z_\phi k^2} \right) + l_{1,1}^{(\text{FB})d} \left(\frac{\rho \bar{h}^2}{Z_L Z_R k^2}, \frac{U' + 2\rho U''}{Z_\phi k^2} \right) \right]. \end{aligned}$$

Switching over to dimensionless quantities, we end up with the representation (25) given in the main text.

3. Flow of the scalar anomalous dimension

For the derivation of the flow of Z_ϕ , we decompose the bosonic field as in App. B 2. The projection of the Wetterich equation onto the massive scalar kinetic term

Plugging this expression into equation (B1), only the term to third power in $\Delta\Gamma_k^{(2)}$ survives the projection. Since we took three derivatives of the Wetterich equation, the diagrammatic interpretation of the result is in terms of one-loop graphs with three external legs: two fermions of opposite chirality and one radial scalar. The gauge contribution comes from triangular loops with three different propagators: one scalar, one spinor and one gauge vector. It always involves the two-scalars-one-vector vertex. This vertex is proportional to the difference of incoming scalar momenta, while the gauge boson propagator in Landau gauge is transverse. These two facts plus conservation of momentum entail that the direct gauge contribution to the momentum-independent Yukawa coupling under consideration vanishes in our truncation. This formal argument can straightforwardly be verified by performing the matrix calculations and taking the supertrace, yielding

$$\partial_t Z_\phi = - \frac{\partial}{\partial(p'^2)} \frac{\delta}{\delta \Delta \phi_1^{\hat{n}}(p')} \frac{\delta}{\delta \Delta \phi_1^{\hat{n}}(q')} \partial_t \Gamma_k \Big|_0.$$

As before the vertical line indicates that the equation is evaluated at vanishing momenta $p' = q' = 0$ and at van-

ishing fluctuation fields. Expanding again the r.h.s. of the flow equation according to eq. (B2), this time only the second order term ($s = 2$) contributes. Since two derivatives of the flow equation have to be taken, the result can diagrammatically be interpreted as one-loop graphs with two external scalar legs. From a one-loop analysis we expect two kinds of gauge contributions. One is due to the two-scalars-one-vector vertex and produces a loop con-

taining one scalar and one gauge boson propagator. This is present in both the symmetric and in the spontaneously broken regimes. Another is due to the two-scalars-two-vectors vertex. If two external scalar legs are identified with the vev, the corresponding loop contains two gauge boson propagators. Therefore this contribution will be present only in the SSB regime. Indeed, performing the matrix calculations and taking the supertrace we find

$$\begin{aligned} \partial_t Z_\phi &= \frac{1}{d} \int \frac{d^d p}{(2\pi)^d} \tilde{\partial}_t \left\{ \left[\left(3\sqrt{2\rho}U'' + 2\sqrt{2\rho^3}U''' \right)^2 p^2 Z_\phi^2 \left(\frac{\frac{\partial}{\partial p^2} P_B}{(Z_\phi P_B + U' + 2\rho U'')^2} \right)^2 + (2N_L - 1) 2\rho U''^2 p^2 Z_\phi^2 \left(\frac{\frac{\partial}{\partial p^2} P_B}{(Z_\phi P_B + U')^2} \right)^2 \right] \right. \\ &+ d_\gamma N_g \bar{h}^2 \left[2p^4 Z_L Z_R \left(\frac{\partial}{\partial p^2} \frac{1+r_L}{Z_L Z_R P_F + \rho \bar{h}^2} \right) \left(\frac{\partial}{\partial p^2} \frac{1+r_R}{Z_L Z_R P_F + \rho \bar{h}^2} \right) - 2\rho \bar{h}^2 p^2 \left(\frac{\partial}{\partial p^2} \frac{1}{Z_L Z_R P_F + \rho \bar{h}^2} \right)^2 \right] \\ &- 4(d-1) \bar{g}^2 Z_\phi^2 \sum_{a=1}^{N_L} \sum_{i=1}^{d_{\text{ad}}} \frac{T_{\hat{n}a}^i T_{a\hat{n}}^i}{(Z_\phi P_B + U')(Z_W P_{\text{GT}} + \bar{m}_{W,i}^2)} \\ &\left. + \frac{(d-1)}{\rho} \sum_{i=1}^{d_{\text{ad}}} \bar{m}_{W,i}^4 \left(\frac{1}{p^2 (Z_W P_{\text{GT}} + \bar{m}_{W,i}^2)^2} + 2p^2 \left(\frac{\partial}{\partial p^2} \frac{1}{Z_W P_{\text{GT}} + \bar{m}_{W,i}^2} \right)^2 \right) \right\}. \end{aligned}$$

Again the whole r.h.s. should be evaluated at the value $\rho = \frac{1}{2}\bar{v}^2$ that minimizes the potential U . Translating this result in terms of threshold functions, yields

$$\begin{aligned} \partial_t Z_\phi &= -\frac{8v_d}{Z_\phi^2 k^{6-d}} \left[\left(3\sqrt{\rho}U'' + 2\sqrt{\rho^3}U''' \right)^2 m_{2,2}^{(\text{B})d} \left(\frac{U'+2\rho U''}{Z_\phi k^2}, \frac{U'+2\rho U''}{Z_\phi k^2} \right) + (2N_L - 1) \rho U''^2 m_{2,2}^{(\text{B})d} \left(\frac{U'}{Z_\phi k^2}, \frac{U'}{Z_\phi k^2} \right) \right] \\ &- \frac{4v_d d_\gamma N_g}{d} \left[\frac{2\bar{h}^2}{Z_L Z_R k^{4-d}} m_4^{(\text{F})d} \left(\frac{\rho \bar{h}^2}{Z_L Z_R k^2} \right) - \frac{2\rho \bar{h}^4}{Z_L^2 Z_R^2 k^{6-d}} m_2^{(\text{F})d} \left(\frac{\rho \bar{h}^2}{Z_L Z_R k^2} \right) \right] \\ &+ \frac{16v_d(d-1)}{d} \frac{\bar{g}^2 Z_\phi}{k^{4-d} Z_W} \sum_{a=1}^{N_L} \sum_{i=1}^{d_{\text{ad}}} T_{\hat{n}a}^i T_{a\hat{n}}^i l_{1,1}^{(\text{BG})d} \left(\frac{U'}{Z_\phi k^2}, \frac{\bar{m}_{W,i}^2}{Z_W k^2} \right) \\ &- \frac{8v_d(d-1)}{d} \sum_{i=1}^{d_{\text{ad}}} \frac{\bar{m}_{W,i}^4}{Z_W^2 k^{6-d} \rho} \left[2a_1^d \left(\frac{\bar{m}_{W,i}^2}{Z_W k^2} \right) + m_2^{(\text{G})d} \left(\frac{\bar{m}_{W,i}^2}{Z_W k^2} \right) \right]. \end{aligned}$$

In terms of dimensionless quantities, this leads to Eq. (26).

4. Flow of the spinor anomalous dimensions

For the anomalous dimensions of the spinors, the procedure is very similar to the one explained for the scalar. In the broken regime, the wave function renormalization of the left-handed spinors in principle splits into two functions. Here we concentrate only on the wave function renormalizations associated with the massive top quark, i.e. those for the \hat{n} -th left-handed component and for the

right-handed one. We start with the projection

$$\partial_t Z_{L/R,k} = \frac{-1}{2v_d d_\gamma N_g} \text{tr} \gamma^\mu \frac{\partial}{\partial p'^\mu} \frac{\overrightarrow{\delta}}{\delta \psi_{L/R}^{\hat{n}}(p')} \partial_t \Gamma_k \frac{\overleftarrow{\delta}}{\delta \psi_{L/R}^{\hat{n}}(q')} \Big|_0$$

where the trace is over spinor and generation indices. As before, the vertical line denotes that the equation is evaluated at vanishing momenta $p' = q' = 0$ and at vanishing fluctuation fields. Expanding the r.h.s. of the flow equation according to Eq. (B2), only the second order term ($s = 2$) contributes. Obviously, the right-handed fermion does not receive direct corrections from the gauge boson whereas the left-handed fermion does. The gauge-field-

independent contributions differ from the results of [7] by a factor of two due to a qualitatively irrelevant prefactor

error in the earlier paper. For the right-handed spinor, the result is

$$\partial_t Z_R = \frac{\bar{h}^2}{d} \int \frac{d^d p}{(2\pi)^d} p^2 \tilde{\partial}_t \left[\frac{Z_R(1+r_R)}{Z_L Z_R P_F + \rho \bar{h}^2} \left(\frac{Z_\phi \frac{\partial}{\partial p^2} P_B}{(Z_\phi P_B + U' + 2\rho U'')^2} + \frac{Z_\phi \frac{\partial}{\partial p^2} P_B}{(Z_\phi P_B + U')^2} \right) + 2(N_L - 1) \frac{Z_R(1+r_R)}{Z_L Z_R P_F} \frac{Z_\phi \frac{\partial}{\partial p^2} P_B}{(Z_\phi P_B + U')^2} \right].$$

In terms of threshold functions, this reads

$$\partial_t Z_R = -\frac{4v_d \bar{h}^2}{d Z_\phi Z_L k^{4-d}} \left[m_{1,2}^{(\text{LB})d} \left(\frac{\rho \bar{h}^2}{Z_L Z_R k^2}, \frac{U'+2\rho U''}{Z_\phi k^2} \right) + m_{1,2}^{(\text{LB})d} \left(\frac{\rho \bar{h}^2}{Z_L Z_R k^2}, \frac{U'}{Z_\phi k^2} \right) + 2(N_L - 1) m_{1,2}^{(\text{LB})d} \left(0, \frac{U'}{Z_\phi k^2} \right) \right],$$

which leads to Eq. (27) in terms of dimensionless quantities. For the left-handed fermion, the result is

$$\begin{aligned} \partial_t Z_L &= \int \frac{d^d p}{(2\pi)^d} \tilde{\partial}_t \left\{ \frac{\bar{h}^2}{d} \frac{Z_L p^2 (1+r_L)}{Z_L Z_R P_F + \rho \bar{h}^2} \left(\frac{Z_\phi \frac{\partial}{\partial p^2} P_B}{(Z_\phi P_B + U' + 2\rho U'')^2} + \frac{Z_\phi \frac{\partial}{\partial p^2} P_B}{(Z_\phi P_B + U')^2} \right) \right. \\ &\quad - \frac{(d-1)}{d} \bar{g}^2 Z_L^2 \sum_{i=1}^{d_{\text{ad}}} (T_{\hat{n}\hat{n}}^i)^2 \left[\left(\frac{2}{Z_W P_{\text{GT}} + \bar{m}_{W,i}^2} + 2p^2 \frac{\partial}{\partial p^2} \frac{1}{Z_W P_{\text{GT}} + \bar{m}_{W,i}^2} \right) \left(\frac{Z_R(1+r_R)}{Z_L Z_R P_F + \rho \bar{h}^2} - \frac{Z_R(1+r_R)}{Z_L Z_R P_F} \right) \right] \\ &\quad \left. - \frac{(d-1)}{d} \bar{g}^2 Z_L^2 \sum_{a=1}^{N_L} \sum_{i=1}^{d_{\text{ad}}} T_{\hat{n}a}^i T_{a\hat{n}}^i \left[\left(\frac{2}{Z_W P_{\text{GT}} + \bar{m}_{W,i}^2} + 2p^2 \frac{\partial}{\partial p^2} \frac{1}{Z_W P_{\text{GT}} + \bar{m}_{W,i}^2} \right) \frac{Z_R(1+r_R)}{Z_L Z_R P_F} \right] \right\}. \end{aligned}$$

In terms of threshold functions, we obtain

$$\begin{aligned} \partial_t Z_L &= -\frac{4v_d \bar{h}^2}{d Z_\phi Z_R k^{4-d}} \left[m_{1,2}^{(\text{RB})d} \left(\frac{\rho \bar{h}^2}{Z_L Z_R k^2}, \frac{U'+2\rho U''}{Z_\phi k^2} \right) + m_{1,2}^{(\text{RB})d} \left(\frac{\rho \bar{h}^2}{Z_L Z_R k^2}, \frac{U'}{Z_\phi k^2} \right) \right] - \frac{8v_d(d-1)}{d} \frac{\bar{g}^2 Z_L}{Z_W k^{4-d}} \left\{ \right. \\ &\quad \sum_{i=1}^{d_{\text{ad}}} (T_{\hat{n}\hat{n}}^i)^2 \left[m_{1,2}^{(\text{LG})d} \left(\frac{\rho \bar{h}^2}{Z_L Z_R k^2}, \frac{\bar{m}_{W,i}^2}{Z_W k^2} \right) - m_{1,2}^{(\text{LG})d} \left(0, \frac{\bar{m}_{W,i}^2}{Z_W k^2} \right) - a_3^d \left(\frac{\rho \bar{h}^2}{Z_L Z_R k^2}, \frac{\bar{m}_{W,i}^2}{Z_W k^2} \right) + a_3^d \left(0, \frac{\bar{m}_{W,i}^2}{Z_W k^2} \right) \right] \\ &\quad \left. + \sum_{a=1}^{N_L} \sum_{i=1}^{d_{\text{ad}}} T_{\hat{n}a}^i T_{a\hat{n}}^i \left[m_{1,2}^{(\text{LG})d} \left(0, \frac{\bar{m}_{W,i}^2}{Z_W k^2} \right) - a_3^d \left(0, \frac{\bar{m}_{W,i}^2}{Z_W k^2} \right) \right] \right\}, \end{aligned}$$

the translation into dimensionless quantities of which agrees with Eq. (28). Upon a global color rotation, we can choose (without loss of generality) the direction of the vev \hat{n} to point along a single color axis, i.e. $\hat{n}^a \propto \delta^{aA}$. Then, this anomalous dimension takes a simpler form, given in Eq. (29).

Appendix C: Flow equation for the gauge coupling

In this appendix, we set the spacetime dimension to $d = 4$, and we focus on the gauge group $\text{SU}(N_L)$. Since we will be satisfied with the one loop beta function we set all the wave function renormalizations to one (terms of order $\mathcal{O}(\partial_t Z)$ on the r.h.s. of the flow equation lead to higher loop corrections of the β_{g^2} function). Still, relevant nonperturbative information will arise from the threshold behavior describing the decoupling of massive modes.

1. Contribution from the gauge modes

For the gauge contribution, the relevant part of the effective Lagrangian is

$$\begin{aligned} \mathcal{L}_k &\ni \frac{1}{4} (F_{\mu\nu}^i)^2 + \bar{g}^2 W_\mu^i W_\mu^j \phi^\dagger T_{ab}^i T_{bc}^j \phi^c + \mathcal{L}_{k,\text{gf}} + \mathcal{L}_{k,\text{gh}} \\ &= \frac{1}{4} (F_{\mu\nu}^i)^2 + \frac{\bar{g}^2 \bar{v}^2}{2} \hat{n}^\dagger T_{ab}^i T_{bc}^j \hat{n}^c W_\mu^i W_\mu^j + \dots \end{aligned}$$

This defines the mass matrix for the gauge bosons, as given in eq. (10). As the generators are real, the mass matrix has real eigenvalues. In order to compute the running coupling, we use the background-field method

and project on the operator $F^2/4$. To the present one-loop order, no distinction between the background field and the fluctuation field has to be made [32, 34], such that it suffices to compute the Hessian $\bar{\Gamma}_k^{(2)}$ at zero fluctuation field. Here and in the following, we use the notation of [32, 35]. This Hessian for the W -boson reads

$$\bar{\Gamma}_k^{(2)ij} \Big|_W = \mathcal{D}_{T\mu\nu}^{ij} + \left(1 - \frac{1}{\alpha}\right) D_\mu^{il} D_\nu^{lj} + \bar{m}_W^2{}^{ij} \delta_{\mu\nu},$$

where $\mathcal{D}_{T\mu\nu} = -D^2 \delta_{\mu\nu} + 2i\bar{g}F_{\mu\nu}$. The contributions from ghost fluctuations are

$$\bar{\Gamma}_k^{(2)ij} \Big|_{gh} = -D_\mu^{il} D_\mu^{lj} + O(\alpha^2) \equiv -(D^2)^{ij} + O(\alpha^2).$$

As we will focus on Landau gauge ($\alpha \rightarrow 0$), we ignore from now on the ghost-Higgs contributions $\sim O(\alpha^2)$. For a covariantly-constant background field, projectors onto the longitudinal and transverse subspaces w.r.t. the background field exist,

$$\Pi_T + \Pi_L = \mathbf{1} \quad , \quad \Pi_{T/L}^2 = \Pi_{T/L} \quad , \quad \Pi_T \Pi_L = 0,$$

with $\Pi_{L\mu\nu} = -(\mathcal{D}_T^{-1})_{\mu\lambda} D_\lambda D_\nu$ and $\Pi_T = \mathbf{1} - \Pi_L$, such that

$$\begin{aligned} \bar{\Gamma}_k^{(2)ij} \Big|_W &= \Pi_T{}^{il}{}_{\mu\lambda} \left[\mathcal{D}_{T\lambda\nu}{}^{lj} + \bar{m}_W^2{}^{ij} \delta_{\lambda\nu} \right] \\ &+ \Pi_L{}^{il}{}_{\mu\lambda} \left[\frac{1}{\alpha} \mathcal{D}_{T\lambda\nu}{}^{lj} + \bar{m}_W^2{}^{ij} \delta_{\lambda\nu} \right] \end{aligned}$$

We choose a similar decomposition for the regulator

$$R_k \Big|_W = \Pi_T \mathcal{D}_T r_k \left(\frac{\mathcal{D}_T}{k^2} \right) + \Pi_L \frac{1}{\alpha} \mathcal{D}_T r_k \left(\frac{\mathcal{D}_T}{k^2} \right)$$

hence also the functional trace on the r.h.s. of the flow equation decomposes into these two sectors. Using the important property that

$$\text{Tr} [\Pi_L f(\mathcal{D}_T)] = \text{Tr} [f(-D^2)],$$

we get

$$\begin{aligned} \text{Tr} \left[\frac{\partial_t R_k}{\Gamma_k^{(2)} + R_k} \right]_W &= \text{Tr} \left[\Pi_T \frac{\mathcal{D}_T \partial_t r_k \left(\frac{\mathcal{D}_T}{k^2} \right)}{\mathcal{D}_T \left(1 + r \left(\frac{\mathcal{D}_T}{k^2} \right) \right) + \bar{m}_W^2} \right] \\ &+ \text{Tr} \left[\frac{(-D^2) \partial_t r_k \left(\frac{-D^2}{k^2} \right)}{(-D^2) \left(1 + r \left(\frac{-D^2}{k^2} \right) \right) + \alpha \bar{m}_W^2} \right] \end{aligned}$$

and writing $\Pi_T = 1 - \Pi_L$ in the first term we obtain two unconstrained traces for different differential operators. The ghost contribution gives

$$\text{Tr} \left[\frac{\partial_t R_k}{\Gamma_k^{(2)} + R_k} \right]_{gh} = -2 \text{Tr} \left[\frac{(-D^2) \partial_t r_k \left(\frac{-D^2}{k^2} \right)}{(-D^2) \left(1 + r \left(\frac{-D^2}{k^2} \right) \right)} \right]$$

such that the total contribution reads in the Landau gauge $\alpha \rightarrow 0$

$$\text{STr} \left[\frac{\partial_t R_k}{\Gamma_k^{(2)} + R_k} \right]_W = \text{Tr} \left[\frac{\mathcal{D}_T \partial_t r_k \left(\frac{\mathcal{D}_T}{k^2} \right)}{\mathcal{D}_T \left(1 + r \left(\frac{\mathcal{D}_T}{k^2} \right) \right) + \bar{m}_W^2} \right] - \text{Tr} \left[\frac{(-D^2) \partial_t r_k \left(\frac{-D^2}{k^2} \right)}{(-D^2) \left(1 + r \left(\frac{-D^2}{k^2} \right) \right) + \bar{m}_W^2} \right] - \text{Tr} \left[\frac{(-D^2) \partial_t r_k \left(\frac{-D^2}{k^2} \right)}{(-D^2) \left(1 + r \left(\frac{-D^2}{k^2} \right) \right)} \right]. \quad (\text{C1})$$

To simplify the calculation, we choose a basis in adjoint color space where the gauge boson mass matrix is diagonal, as in Eq. (11), and we also specify a constant pseudo-abelian magnetic background field

$$F_{\mu\nu}^i = \hat{m}^i F_{\mu\nu} \quad , \quad \hat{m}_i \hat{m}^i = 1 \quad , \quad F_{\mu\nu} = B \epsilon_{\mu\nu}^\perp$$

where \hat{m} is a unit vector pointing into a direction in the Cartan of the algebra. The constant antisymmetric tensor ϵ characterizes the space directions which are affected by the constant magnetic field upon the Lorentz force. Recalling that the adjoint generators are $(\tau^l)_{ij} = i f^{ilj}$, we choose a basis in adjoint color space, such that $i f^{ilj} \hat{m}^l$ is diagonal with eigenvalues ν_i . Then, the covariant derivative

$$D_\mu^{ij} = (\partial_\mu - i\nu_i) \delta^{ij} \quad (\text{no sum over } i) \quad (\text{C2})$$

is also diagonal, and so are D^2 and \mathcal{D}_T . Hence \mathcal{D}_T and \bar{m}_W^2 commute, as well as D^2 and \bar{m}_W^2 . Equation (C1)

can thus be brought into proper-time form:

$$\begin{aligned} \text{STr} \left[\frac{\partial_t R_k}{\Gamma_k^{(2)} + R_k} \right]_W &= - \int_0^\infty ds \tilde{h}(s, 0) \text{Tr} \left[e^{-s \frac{-D^2}{k^2}} \right] \\ &+ \int_0^\infty ds \text{Tr} \left[\tilde{h}(s, m_W^2) \left(e^{-s \frac{\mathcal{D}_T}{k^2}} - e^{-s \frac{-D^2}{k^2}} \right) \right] \end{aligned}$$

where \tilde{h} is the Laplace transform of the function

$$h(y, m_W^2) = \frac{y \partial_t r_k(y)}{y(1 + r_k(y)) + m_W^2}$$

with respect to y , that is

$$h(y, m_W^2) = \int_0^\infty ds \tilde{h}(s, m_W^2) e^{-sy},$$

where as before $m_W^2 = \bar{m}_W^2/k^2$. The heat kernel traces are known, see [35]

$$\begin{aligned} \text{Tr} \left[\tilde{h}(s, m_W^2) e^{-s \frac{D^2}{k^2}} \right] &= \frac{\Omega k^4}{4\pi^2 s^2} \sum_{i=1}^{d_{\text{ad}}} \tilde{h}(s, m_{W,i}^2) \\ &\quad \times \left\{ \frac{\frac{sb_i}{k^2}}{\sinh\left(\frac{sb_i}{k^2}\right)} + \frac{sb_i}{k^2} \sinh\left(\frac{sb_i}{k^2}\right) \right\} \\ \text{Tr} \left[\tilde{h}(s, m_W^2) e^{-s \frac{D^2}{k^2}} \right] &= \frac{\Omega k^4}{16\pi^2 s^2} \sum_{i=1}^{d_{\text{ad}}} \tilde{h}(s, m_{W,i}^2) \frac{\frac{sb_i}{k^2}}{\sinh\left(\frac{sb_i}{k^2}\right)} \\ \text{Tr} \left[\tilde{h}(s, 0) e^{-s \frac{D^2}{k^2}} \right] &= \frac{\Omega k^4}{16\pi^2 s^2} \sum_{i=1}^{d_{\text{ad}}} \tilde{h}(s, 0) \frac{\frac{sb_i}{k^2}}{\sinh\left(\frac{sb_i}{k^2}\right)} \end{aligned} \quad (\text{C3})$$

where $b_i = \bar{g}|\nu_i|B$ and Ω is the spacetime volume. The first trace above is over spacetime and Lorentz and color indices, the other two only over spacetime and color indices. For the running gauge coupling we just need the terms of order b_i^2 , since the relevant term on the l.h.s. of the flow equation is $\partial_t \Gamma_k \ni \Omega B^2 \partial_t Z_W / 2$. Using that the running of the renormalized coupling g^2 is given in terms of the anomalous dimension, $\partial_t g^2 = \beta_{g^2} = \eta_W g^2$, we find

$$\eta_W \Big|_W = \frac{-g^2}{32\pi^2} \sum_{i=1}^{d_{\text{ad}}} [21h(0, m_{W,i}^2) + h(0, 0)] \frac{|\nu_i|^2}{3}. \quad (\text{C4})$$

In the background-field method, the $y \rightarrow 0$ limit of the regulator is constrained [34, 35]; the only regulators permitted must satisfy $h(y \rightarrow 0, 0) = 2$. In the massless limit we thus obtain

$$\eta_W \Big|_W = -\frac{1}{16\pi^2} \frac{22}{3} g^2 \sum_{i=1}^{d_{\text{ad}}} |\nu_i|^2 = -\frac{1}{16\pi^2} \frac{22}{3} g^2 N_L,$$

which agrees with standard perturbation theory. Let us work out the massive case using the linear regulator (A2). In this case, $h(y, x) = 2(1+x)^{-1}\theta(1-y)$, such that the gauge contribution to the gauge β_{g^2} function reads

$$\beta_{g^2} \Big|_W = \eta_W \Big|_W g^2 = -\frac{g^4}{16\pi^2} \left[\frac{21}{3} \sum_{i=1}^{d_{\text{ad}}} \frac{|\nu_i|^2}{1+m_{W,i}^2} + \frac{N_L}{3} \right].$$

The first term now depends on the choice of \hat{n}^a the direction of the vev in fundamental color space. This is expected, as for higher gauge groups different breaking patterns and gauge masses can arise. This term also depends in general on $|\nu_i|^2$, i.e. on \hat{m}^i . This is also plausible, as the directions of the vev implicitly also allows for the definition of different couplings: depending on the relative direction of the gauge fluctuation w.r.t. the vev, the fluctuations can couple differently to matter.

For SU(2), these issues simplify, as

$$\bar{m}_W^2{}^{ij} = \frac{\bar{g}^2 \bar{v}^2}{4} \hat{n}^{\dagger a} \sigma_{ab}^i \sigma_{bc}^j \hat{n}^c = \frac{\bar{g}^2 \bar{v}^2}{4} (\delta^{ij} + i\epsilon^{ijl} (\hat{n}^{\dagger} \sigma^l \hat{n})), \quad (\text{C5})$$

such that $\text{tr} \bar{m}_W^2{}^{ij} = 3\bar{g}^2 \bar{v}^2 / 4$. Let us denote $c^l = (\hat{n}^{\dagger} \sigma^l \hat{n})$. This is a vector in adjoint space which is an eigenvector of the mass matrix, with eigenvalue $\bar{g}^2 \bar{v}^2 / 4$. One can choose a diagonalizing orthonormal basis $\{e_1, e_2 = c/|c|, e_3\}$ in adjoint space such that the mass matrix takes the form

$$\bar{m}_W^2 = \frac{\bar{g}^2 \bar{v}^2}{4} \begin{pmatrix} 2 & 0 & 0 \\ 0 & 1 & 0 \\ 0 & 0 & 0 \end{pmatrix}.$$

Now recall that the ν_i denotes the eigenvalues of $(-i f^{ijl} \hat{m}^l)$, that for SU(2) simply is $(-i\epsilon^{ijl} \hat{m}^l)$. Therefore in SU(2) the eigenvalues are $(1, -1, 0)$ for any choice of \hat{m} . However, depending on the direction of \hat{m} w.r.t. the basis defined above, the ν_i could be $\{\nu_1 = 1, \nu_2 = -1, \nu_3 = 0\}$ or possibly permutations thereof. The two extreme cases for SU(2) are maximal or minimal decoupling. Maximal decoupling happens if $|\nu_1| = |\nu_2| = 1$ and $\nu_3 = 0$, and in this case

$$\beta_{g^2} \Big|_W = -\frac{g^4}{16\pi^2} \left[\frac{21}{3} \left(\frac{1}{1 + \frac{g^2 v^2}{2k^2}} + \frac{1}{1 + \frac{g^2 v^2}{4k^2}} \right) + \frac{2}{3} \right] \quad (\text{C6})$$

while minimal decoupling happens if $\nu_1 = 0$ and $|\nu_2| = |\nu_3| = 1$, and correspondingly

$$\beta_{g^2} \Big|_W = -\frac{g^4}{16\pi^2} \left[\frac{21}{3} \left(1 + \frac{1}{1 + \frac{g^2 v^2}{4k^2}} \right) + \frac{2}{3} \right]. \quad (\text{C7})$$

For SU(2) the ambiguity of the β -function arises solely from the ambiguity of defining a coupling in the presence of a vev. In fact, there are more quadratic invariants than the only F^2 , such as for example $\hat{n}^{\dagger a} F_{\mu\nu}^i T_{ab}^i T_{bc}^j F_{\mu\nu}^j \hat{n}^c$. For higher groups, even the mass matrix depends on the choice of \hat{n}^a .

2. Contribution from scalar modes

The contribution from scalar fluctuations to the gauge β function arises from the scalar kinetic term. The calculation is very similar to that of the longitudinal gauge modes with two differences: the field is complex and lives in the fundamental representation. Moreover the dimensionless scalar mass matrix in the broken regime reads $m_\phi^2{}^{ab} = (\lambda_2 v^2 / 2k^2) \hat{n}^a \hat{n}^{\dagger b}$. Here, we do not attempt to solve the problem in full generality as for the gauge modes, but confine ourselves to a simple choice of backgrounds. Most importantly, we choose the direction of the pseudo abelian background to satisfy

$$W_\mu^i = \hat{m}^i W_\mu, \quad \hat{m}_i \hat{m}^i = 1, \quad [(\hat{m}_i T^i), \hat{n} \otimes \hat{n}^{\dagger}] = 0. \quad (\text{C8})$$

It is important to note that this does not constrain the choice of the vev-direction \hat{n}^a . This is because we can always choose a basis in fundamental color space such that the projector $P_{\hat{n}} = \hat{n} \otimes \hat{n}^{\dagger}$ is diagonal. Then the

commutation relation (C8) can be satisfied by choosing $(\hat{m}_i T^i)^{ab}$ to be in the Cartan, i.e. by choosing it to be diagonal in that basis.

Let's consider SU(2) as an example. Let $\hat{n} = (0, 1)$. Then we choose $\hat{m} = (0, 0, 1)$ such that

$$(\hat{m}_i T^i)^{ab} = \frac{1}{2}\sigma^3 = \frac{1}{2} \begin{pmatrix} 1 & 0 \\ 0 & -1 \end{pmatrix}, \quad (\text{C9})$$

obviously satisfying Eq. (C8). Before we continue with the scalar fluctuations, let us work out the consequences of this choice for the gauge modes of the preceding section. The vector c for this choice becomes $c = (0, 0, -1)$ and the mass matrix for the gauge modes, given by (C5), is

$$\bar{m}_W^2{}^{ij} = \frac{\bar{g}^2 \bar{v}^2}{4} (\delta^{ij} - i\epsilon^{ij3}) = \frac{\bar{g}^2 \bar{v}^2}{4} \begin{pmatrix} 1 & -i & 0 \\ i & 1 & 0 \\ 0 & 0 & 1 \end{pmatrix}. \quad (\text{C10})$$

The definition of ν_i , right above (C2), combined with the choice $\hat{m} = (0, 0, 1)$ requires us to compute the eigenvalues of

$$-i\epsilon^{ij3} = -i \begin{pmatrix} 0 & 1 & 0 \\ -1 & 0 & 0 \\ 0 & 0 & 0 \end{pmatrix}.$$

The simultaneous eigenvectors of this matrix and of \bar{m}_W^2 are given by

$$v_1 = \begin{pmatrix} 0 \\ 0 \\ 1 \end{pmatrix}, \quad v_2 = \begin{pmatrix} 1 \\ i \\ 0 \end{pmatrix}, \quad v_3 = \begin{pmatrix} 1 \\ -i \\ 0 \end{pmatrix}$$

with the corresponding set of eigenvalues: $\{\bar{m}_{W,1}^2 = \frac{\bar{g}^2 \bar{v}^2}{4}, \nu_1 = 0\}$, $\{\bar{m}_{W,2}^2 = \frac{\bar{g}^2 \bar{v}^2}{2}, \nu_2 = 1\}$, $\{\bar{m}_{W,3}^2 = 0, \nu_3 = -1\}$. This choice of \hat{m} corresponds to the minimal decoupling case of Eq. (C7). These considerations tell us that the maximal decoupling solution of Eq. (C6) might not be permitted, as it would not correspond to a legitimate choice of \hat{m} with $\hat{m}_i T^i$ in the Cartan (which we had also assumed in the gluonic case in eq. (C2)). The choice (C8) for defining \hat{m} therefore is related to defining the coupling with respect to the unbroken part of the gauge group.

Let us now return to the scalar fluctuations; Eq. (C8) ensures that the covariant derivative in the fundamental representation satisfies

$$[D_\mu, \hat{n} \otimes \hat{n}^\dagger] = 0$$

for our choice of the background field. Then also $[-D^2, \hat{n} \otimes \hat{n}^\dagger] = 0$ and thus $[-D^2, m_\phi^2] = 0$ follow, such that $-D^2$ and m_ϕ^2 can be simultaneously diagonalized. Therefore

$$\text{Tr} \left[\frac{\partial_t R_k}{\Gamma^{(2)} + R_k} \right]_\phi = \text{Tr} \left[\frac{\frac{-D^2}{k^2} \partial_t r_k \left(\frac{-D^2}{k^2} \right)}{\frac{-D^2}{k^2} (1 + r_k \left(\frac{-D^2}{k^2} \right)) + m_\phi^2} \right].$$

Because of the above considerations, we can rewrite the previous expression in the proper time form

$$\begin{aligned} \text{Tr} \left[\frac{\partial_t R_k}{\Gamma^{(2)} + R_k} \right]_\phi &= \int_0^\infty ds \text{Tr} \left[\tilde{h}(s, m_\phi^2) e^{-s \frac{-D^2}{k^2}} \right] \\ &= \frac{\Omega}{16\pi^2} \int_0^\infty ds \sum_{a=1}^{N_L} \tilde{h}(s, m_{\phi,a}^2) \left(-\frac{1}{6} b_a^2 \right), \end{aligned}$$

where we have retained only the term of order b_a^2 (compare with the second equation of (C3)). We have denoted the eigenvalues of the mass matrix by $m_{\phi,a}^2$ (there is only one nonvanishing eigenvalue for the radial mode). Furthermore, $b_a = \bar{g} |\nu_a| B$, where ν_a now are the eigenvalues of $(\hat{m}_i T^i)^{ab}$ related to the fundamental representation. Using the standard normalization for the generators of the fundamental representation, we have

$$\sum_{a=1}^{N_L} |\nu_a|^2 = \text{tr} \left[(\hat{m}_i T^i)^2 \right] = \hat{m}_i \hat{m}_j \frac{1}{2} \delta^{ij} = \frac{1}{2}.$$

Another difference from the gauge case is that the scalar field is complex and thus there is no factor 1/2 in front of the trace on the r.h.s. of the flow equation. Hence, analogous to (C4), the contribution of the scalar to the flow of Z_W reads

$$\eta_W \Big|_\phi = \frac{g^2}{16\pi^2} \sum_{a=1}^{N_L} h(0, m_{\phi,a}^2) \frac{|\nu_a|^2}{3}. \quad (\text{C11})$$

In the massless case, since $h(0, 0) = 2$, $\eta_W \Big|_\phi = \frac{g^2}{16\pi^2} \frac{1}{3}$ in agreement with perturbation theory. In the general massive case and using the linear regulator, we get

$$\eta_W \Big|_\phi = \frac{g^2}{16\pi^2} \frac{2}{3} \sum_{a=1}^{N_L} \frac{1}{1 + m_{\phi,a}^2} |\nu_a|^2.$$

Generically, only one particular component of $m_{\phi,a}^2$ is nonvanishing and equal to $2\lambda_2 \kappa$. For SU(2) the ν_a are unique and equal to $\{\frac{1}{2}, -\frac{1}{2}\}$. Therefore in this case

$$\eta_W \Big|_\phi = \frac{g^2}{16\pi^2} \frac{1}{3} \left[\frac{1}{2} + \frac{1}{2} \frac{1}{1 + 2\lambda_2 \kappa} \right].$$

3. Contribution from fermion modes

The relevant part of the effective Lagrangian is

$$\mathcal{L}_k \ni i(\bar{\psi}_L^a \not{D}^{ab} \psi_L^b + \bar{\psi}_R \not{D} \psi_R) + \bar{h}(\bar{\psi}_R \phi^{a\dagger} \psi_L^a - \bar{\psi}_L^a \phi^a \psi_R),$$

where again we have set any wave function renormalization to one. For Eq. (6), we can choose a gauge background field such that D_μ^{ab} and $P_{\hat{n}} = \hat{n} \otimes \hat{n}^\dagger$ as well as $P_{(1-\hat{n})} = 1 - P_{\hat{n}}$ commute and the above parts of \mathcal{L}_k can be written as

$$\begin{aligned} \mathcal{L}_k \ni & i(\bar{\psi}_L^a \not{D}^{ab} P_{(1-\hat{n})}^{bc} \psi_L^c) \\ & + i(\bar{\psi}_L^{\hat{n}} \not{D} \psi_L^{\hat{n}} + \bar{\psi}_R \not{D} \psi_R) + \frac{\bar{h}\bar{v}}{\sqrt{2}} (\bar{\psi}_R \psi_L^{\hat{n}} - \bar{\psi}_L^{\hat{n}} \psi_R) \end{aligned} \quad (\text{C12})$$

Here, the \not{D} in the second term is projected along \hat{n} . The first line corresponds to the massless bottom-type fermions. Their contribution is the standard perturbative contribution weighted by eigenvalues ν_a in the orthogonal complement. Let \hat{n} point into the A -direction: $\hat{n}^a = \delta^{aA}$. Then the contribution of the massless fermions to the running coupling is

$$\partial_t g^2 \Big|_{\psi_{(1-\hat{n})}} = \frac{g^4}{16\pi^2} \frac{2d_\gamma N_g}{3} \sum_{a=1, a \neq A}^{N_L} |\nu_a|^2.$$

If the sum ran over all a 's we would get $\sum_{a=1}^{N_L} |\nu_a|^2 = 1/2$ leading to the correct perturbative result. Combining $\psi_L^{\hat{n}}$ and ψ_R into a Dirac spinor $\Psi = \begin{pmatrix} \psi_L^{\hat{n}} \\ \psi_R \end{pmatrix}$, the second line of (C12) can be written

$$\mathcal{L}_k \ni i\bar{\Psi} \not{D}_{AL} \Psi + \bar{m}_t \bar{\Psi} \gamma_5 \Psi$$

where $\not{D}_{AL} = \gamma_\mu (\partial^\mu - \bar{g} \nu_A W^\mu P_L)$, with the usual definition of the left projector $P_L = \frac{1}{2}(1 - \gamma_5)$. We have also introduced the ‘‘top-mass’’ \bar{m}_t as defined in eq. (12). Since the regularized fluctuation operator for Ψ satisfies $(\Gamma_k^{(2)} + R_k) = \not{D}_{AL}(1 + r_k) + \bar{m}_t \gamma_5$ and since $\text{tr}[\gamma_5 \not{D}_{AL}] = 0$, we get

$$\begin{aligned} \text{Tr} \left[\frac{\partial_t R_k}{\Gamma^{(2)} + R_k} \right]_\Psi &= \text{Tr} \left[\frac{\not{D}_{AL}^2 \left(1 + r_k \left(\frac{\not{D}_{AL}^2}{k^2} \right) \right) \partial_t r \left(\frac{\not{D}_{AL}^2}{k^2} \right)}{\not{D}_{AL}^2 \left(1 + r_k \left(\frac{\not{D}_{AL}^2}{k^2} \right) \right)^2 + \bar{m}_t^2} \right] \\ &= \int_0^\infty ds \tilde{h}(s, \bar{m}_t^2) \text{Tr} \left[e^{-s \frac{\not{D}_{AL}^2}{k^2}} \right] \end{aligned} \quad (\text{C13})$$

Here we need to know the spectrum of

$$\begin{aligned} \not{D}_{AL}^2 &= \gamma_\mu (\partial^\mu - \bar{g} \nu_A W^\mu P_L) \gamma_\nu (\partial^\nu - \bar{g} \nu_A W^\nu P_L) = \gamma_\mu \gamma_\nu (\partial^\mu - \bar{g} \nu_A W^\mu P_R) (\partial^\nu - \bar{g} \nu_A W^\nu P_L) \\ &= \gamma_\mu \gamma_\nu (D_R^\mu + \partial_L^\mu) (D_L^\nu + \partial_R^\nu) = \not{D}_L^2 + \gamma_\mu \gamma_\nu (\partial_L^\mu D_L^\nu + D_R^\mu \partial_R^\nu) \end{aligned} \quad (\text{C14})$$

where we have denoted $\partial_{L/R}^\mu = \partial^\mu P_{L/R}$ and took advantage of: $\not{D}_L^2 = \gamma_\mu \gamma_\nu D_R^\mu D_L^\nu$ and $\partial_L^\mu \partial_R^\nu = 0$. The determination of this spectrum probably is an analytically solvable problem for a constant magnetic field background, as the differential operator is of harmonic oscillator type, however, with an involved Dirac structure.

As we are mainly interested in the decoupling of massive modes in the flow of the gauge coupling, let us simply take a shortcut at this point. We already know that the contribution of Eq. (C13) to the β -function in the massless limit must be of the form

$$\partial_t g^2 \Big|_{\psi_{\hat{n}}} = \frac{g^4}{16\pi^2} \frac{2d_\gamma N_g}{3} |\nu_A|^2.$$

This fixes the $\mathcal{O}(s^0)$ -term in $\text{Tr} \left[e^{-s \frac{\not{D}_{AL}^2}{k^2}} \right]$ to be the same as the $\mathcal{O}(s^0)$ -term in $\text{Tr} \left[e^{-s \frac{\not{D}_L^2}{k^2}} \right]$. These heat-kernel traces could still differ to higher orders in s , due to the two extra terms in (C14). These higher-order terms could (unlike as for \not{D}_L^2) in principle contain terms of order B^2 and thus contribute to the beta function via functions of the form

$$f_p(m_t^2) = \int_0^\infty ds \tilde{h}(s, m_t^2) s^p = \left[\left(-\frac{\partial}{\partial y} \right)^p h(y, m_t^2) \right]_{y=0}$$

where m_t^2 is the dimensionless top mass squared: $m_t^2 = h^2 \kappa$. Because of the constraints from the massless limit

discussed before, we must have $f_p(0) = 0$. Furthermore f_p also has to exhibit a generic threshold behavior, that is: $f_p(m_t^2 \rightarrow \infty) \rightarrow 0$. As the precise dependence of $h(0, m_t^2)$ is anyway regulator-dependent, we simply ignore potentially nonvanishing contributions of $f_p(m_t^2)$ for all practical discussions in the main text. Therefore, without any further explicit calculation, we approximate the threshold behavior of the massive fermion mode by the same form as for the other modes

$$\partial_t g^2 \Big|_\psi = \frac{g^4}{16\pi^2} \frac{2d_\gamma N_g}{3} \sum_{a=1}^{N_L} \frac{1}{1 + h^2 \kappa \delta^{aA}} |\nu_a|^2.$$

For SU(2) this implies

$$\partial_t g^2 \Big|_\psi = \frac{g^4}{16\pi^2} \frac{d_\gamma N_g}{3} \left(\frac{1}{2} + \frac{1}{2} \frac{1}{1 + h^2 \kappa} \right).$$

To summarize, we can write the gauge one-loop β -function approximately as given in the main text in eqs. (30,31).

Appendix D: Results for the anomaly-free two-generation model $N_g = 2$

In this appendix, we verify explicitly that the properties of the anomaly-free SU($N_L = 2$) model with two

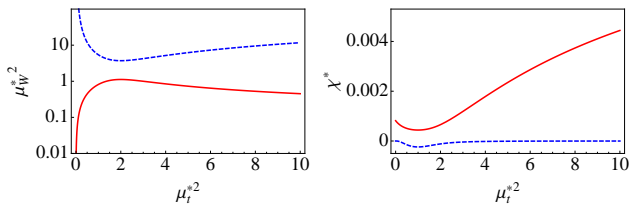


FIG. 6: Fixed point values for μ_W^2 (left panel) and χ (right panel) as a function of the fixed point value of μ_t^2 for $N_L = 2$ and $N_g = 2$. This shows the similarity to the one-generation case depicted in Fig. 2.

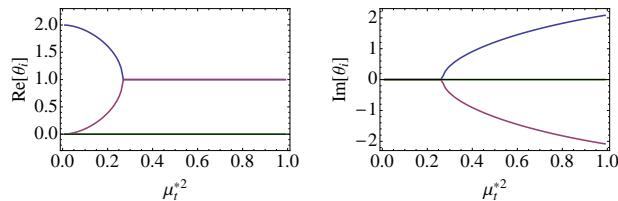


FIG. 7: Critical exponents for the line of fixed points computed in the mass parametrization as a function of the fixed point top mass parameter μ_t^{*2} for $N_L = 2$ and $N_g = 2$; left panel: real parts, right panel: imaginary parts. Again the similarity to the one-generation case, c.f., Fig. 3 is obvious.

left-handed generations $N_g = 2$ are essentially identical to the results for the one-generation model discussed in the main text. This can be seen manifestly by comparing Figs. 6, 7, where $N_g = 2$, to Figs. 2, 3, where $N_g = 1$. These explicit solutions verify that the transition from one generation to two generations induces only small quantitative differences in the fixed-point values as well as in the values for the critical exponents.

We emphasize again that the $N_g = 1$ model discussed in the main text for phenomenological reasons has a Witten anomaly and thus should be considered as embedded into a larger anomaly free model, such as the standard model. By contrast, with the results of this appendix, we conclude that the $N_g = 2$ model as it stands can be a consistent UV complete quantum field theory for all trajectories emanating from the line of non-Gaussian fixed points.

-
- [1] K. G. Wilson and J. B. Kogut, Phys. Rept. **12**, 75 (1974); M. Luscher and P. Weisz, Nucl. Phys. B **295**, 65 (1988); Nucl. Phys. B **318**, 705 (1989); A. Hasenfratz, K. Jansen, C. B. Lang, T. Neuhaus and H. Yoneyama, Phys. Lett. B **199**, 531 (1987); U. M. Heller, H. Neuberger and P. M. Vranas, Nucl. Phys. B **399**, 271 (1993) [arXiv:hep-lat/9207024]; D. J. E. Callaway, Phys. Rept. **167**, 241 (1988); O. J. Rosten, JHEP **0907**, 019 (2009) [arXiv:0808.0082 [hep-th]].
- [2] L.D. Landau, in *Niels Bohr and the Development of Physics*, ed. W. Pauli, Pergamon Press, London, (1955).
- [3] M. Gell-Mann and F. E. Low, Phys. Rev. **95**, 1300 (1954).
- [4] M. Goeckeler, R. Horsley, V. Linke, P. Rakow, G. Schierholz and H. Stuben, Phys. Rev. Lett. **80**, 4119 (1998); Nucl. Phys. Proc. Suppl. **63** (1998) 694.
- [5] H. Gies and J. Jaeckel, Phys. Rev. Lett. **93**, 110405 (2004) [arXiv:hep-ph/0405183].
- [6] H. Gies and M. M. Scherer, Eur. Phys. J. C **66**, 387 (2010) [arXiv:0901.2459 [hep-th]].
- [7] H. Gies, S. Rechenberger and M. M. Scherer, Eur. Phys. J. C **66**, 403 (2010) [arXiv:0907.0327 [hep-th]]; M. M. Scherer, H. Gies and S. Rechenberger, Acta Phys. Polon. Supp. **2**, 541 (2009) [arXiv:0910.0395 [hep-th]].
- [8] W. Wetzel, Nucl. Phys. B **196**, 259 (1982); W. Bernreuther and W. Wetzel, Nucl. Phys. B **197**, 228 (1982) [Erratum-ibid. B **513**, 758 (1998)].
- [9] Y. Schroder and M. Steinhauser, JHEP **0601**, 051 (2006) [hep-ph/0512058].
- [10] S. Weinberg, in *C76-07-23.1 HUTP-76/160*, Erice Subnucl. Phys., 1, (1976).
- [11] K. G. Wilson, Phys. Rev. D **7**, 2911 (1973); B. Rosenstein, B. J. Warr and S. H. Park, Phys. Rev. Lett. **62**, 1433 (1989); K. Gawedzki and A. Kupiainen, Phys. Rev. Lett. **55**, 363 (1985); C. de Calan, P. A. Faria da Veiga, J. Magnen and R. Seneor, Phys. Rev. Lett. **66**, 3233 (1991);
- [12] J. Braun, H. Gies and D. D. Scherer, Phys. Rev. D **83**, 085012 (2011) [arXiv:1011.1456 [hep-th]].
- [13] G. Parisi, Nucl. Phys. B **100**, 368 (1975); S. Hands, Phys. Rev. D **51**, 5816 (1995) [hep-th/9411016]; S. Christofi, S. Hands and C. Strouthos, Phys. Rev. D **75**, 101701 (2007) [hep-lat/0701016]; H. Gies and L. Janssen, Phys. Rev. D **82**, 085018 (2010) [arXiv:1006.3747 [hep-th]]; L. Janssen, www.db-thueringen.de/servlets/DocumentServlet?id=20856, PhD thesis, Jena U. (2012).
- [14] S. Chandrasekharan and A. Li, Phys. Rev. Lett. **108**, 140404 (2012) [arXiv:1111.7204 [hep-lat]]; arXiv:1304.7761 [hep-lat].
- [15] M. Reuter, Phys. Rev. D **57**, 971 (1998) [arXiv:hep-th/9605030]; O. Lauscher and M. Reuter, Phys. Rev. D **65**, 025013 (2002) [arXiv:hep-th/0108040]; Class. Quant. Grav. **19**, 483 (2002) [arXiv:hep-th/0110021]; W. Souma, Prog. Theor. Phys. **102**, 181 (1999) [arXiv:hep-th/9907027]; P. Forgacs and M. Niedermaier, arXiv:hep-th/0207028;

- R. Percacci and D. Perini, Phys. Rev. D **67**, 081503 (2003) [arXiv:hep-th/0207033]; A. Codello, R. Percacci and C. Rahmede, Int. J. Mod. Phys. A **23**, 143 (2008) [arXiv:0705.1769 [hep-th]]; M. Reuter and F. Saueressig, New J. Phys. **14**, 055022 (2012).
- [16] R. Percacci and D. Perini, Phys. Rev. D **68**, 044018 (2003) [hep-th/0304222]; A. Eichhorn, Phys. Rev. D **86**, 105021 (2012) [arXiv:1204.0965 [gr-qc]].
- [17] O. Zanusso, L. Zambelli, G. P. Vacca and R. Percacci, Phys. Lett. B **689**, 90 (2010) [arXiv:0904.0938 [hep-th]]; G. P. Vacca and O. Zanusso, Phys. Rev. Lett. **105**, 231601 (2010) [arXiv:1009.1735 [hep-th]].
- [18] A. Eichhorn and H. Gies, New J. Phys. **13**, 125012 (2011) [arXiv:1104.5366 [hep-th]].
- [19] U. Harst and M. Reuter, JHEP **1105**, 119 (2011) [arXiv:1101.6007 [hep-th]].
- [20] H. Gies, J. Jaeckel and C. Wetterich, Phys. Rev. D **69**, 105008 (2004) [arXiv:hep-ph/0312034].
- [21] F. Bazzocchi, M. Fabbrichesi, R. Percacci, A. Tonero and L. Vecchi, Phys. Lett. B **705**, 388 (2011) [arXiv:1105.1968 [hep-ph]].
- [22] J. M. Schwindt and C. Wetterich, arXiv:0812.4223 [hep-th].
- [23] S. Kim, A. Kocic and J. B. Kogut, Nucl. Phys. B **429**, 407 (1994) [hep-lat/9402016].
- [24] J. Zinn-Justin, Nucl. Phys. B **367**, 105 (1991).
- [25] A. Hasenfratz, P. Hasenfratz, K. Jansen, J. Kuti and Y. Shen, Nucl. Phys. B **365**, 79 (1991).
- [26] F. Englert and R. Brout, Phys. Rev. Lett. **13**, 321 (1964); P. W. Higgs, Phys. Lett. **12**, 132 (1964); Phys. Rev. Lett. **13**, 508 (1964); G. S. Guralnik, C. R. Hagen and T. W. B. Kibble, Phys. Rev. Lett. **13**, 585 (1964).
- [27] R. D. Ball, Phys. Rept. **182**, 1 (1989).
- [28] E. Witten, Phys. Lett. B **117**, 324 (1982).
- [29] C. Wetterich, Phys. Lett. B **301**, 90 (1993).
- [30] D. F. Litim and J. M. Pawłowski, in *The Exact Renormalization Group*, Eds. Krasnitz et al, World Sci 168 (1999); J. M. Pawłowski, Ann. Phys. **322**, 2831 (2007) [hep-th/0512261]; H. Gies, Lect. Notes Phys. **852**, 287 (2012) [hep-ph/0611146];
- [31] K. Aoki, Int. J. Mod. Phys. B **14**, 1249 (2000); J. Berges, N. Tetradis and C. Wetterich, Phys. Rept. **363**, 223 (2002) [hep-ph/0005122]; B. Delamotte, Lect. Notes Phys. **852**, 49 (2012) [cond-mat/0702365 [COND-MAT]]; P. Kopietz, L. Bartosch and F. Schutz, Lect. Notes Phys. **798**, 1 (2010); J. Braun, J. Phys. G **39**, 033001 (2012) [arXiv:1108.4449]; S. Nagy, arXiv:1211.4151 [hep-th].
- [32] M. Reuter and C. Wetterich, Nucl. Phys. B **417**, 181 (1994) arXiv:hep-th/9411227; Phys. Rev. D **56** (1997) 7893 [hep-th/9708051].
- [33] U. Ellwanger, Phys. Lett. B **335**, 364 (1994) [hep-th/9402077];
- [34] J. M. Pawłowski, Int. J. Mod. Phys. A **16** (2001) 2105; Acta Physica Slovaca **52** (2002) 475; D. F. Litim and J. M. Pawłowski, Phys. Lett. B **546**, 279 (2002) [hep-th/0208216]; F. Freire, D. Litim and J. M. Pawłowski, Phys. Lett. B, **495**, 256-262 (2000).
- [35] H. Gies, Phys. Rev. D **66** (2002) 025006 [hep-th/0202207].
- [36] V. Branchina, K. A. Meissner and G. Veneziano, Phys. Lett. B **574** (2003) 319 [hep-th/0309234]; J. M. Pawłowski, hep-th/0310018.
- [37] L. F. Abbott, Nucl. Phys. B **185**, 189 (1981); W. Dittrich and M. Reuter, Lect. Notes Phys. **244**, 1 (1986).
- [38] J. Frohlich, G. Morchio and F. Strocchi, Nucl. Phys. B **190**, 553 (1981).
- [39] A. Maas, arXiv:1205.6625 [hep-lat]; A. Maas and T. Mufti, arXiv:1211.5301 [hep-lat].
- [40] U. Ellwanger, M. Hirsch and A. Weber, Z. Phys. C **69**, 687 (1996) [hep-th/9506019]; D. F. Litim and J. M. Pawłowski, Phys. Lett. B **435**, 181 (1998) [hep-th/9802064].
- [41] D. F. Litim, Phys. Lett. B **486**, 92 (2000) [hep-th/0005245]; Phys. Rev. D **64**, 105007 (2001) [hep-th/0103195].
- [42] S. Weinberg, In *Hawking, S.W., Israel, W.: General Relativity**, 790-831; M. Reuter, Phys. Rev. D **57**, 971 (1998) [arXiv:hep-th/9605030]; M. Niedermaier and M. Reuter, Living Rev. Rel. **9**, 5 (2006); R. Percacci, In **Orti, D. (ed.): Approaches to quantum gravity** 111-128 [arXiv:0709.3851 [hep-th]]; M. Reuter and F. Saueressig, New J. Phys. **14**, 055022 (2012) [arXiv:1202.2274 [hep-th]].
- [43] D. F. Litim, J. M. Pawłowski and L. Vergara, hep-th/0602140.
- [44] L. Maiani, G. Parisi and R. Petronzio, Nucl. Phys. B **136**, 115 (1978); M. Lindner, Z. Phys. C **31**, 295 (1986). T. Hambye and K. Riesselmann, Phys. Rev. D **55**, 7255 (1997) [hep-ph/9610272]; G. Altarelli and G. Isidori, Phys. Lett. B **337**, 141 (1994); J. A. Casas, J. R. Espinosa and M. Quiros, Phys. Lett. B **342**, 171 (1995) [hep-ph/9409458]; G. Degrassi, S. Di Vita, J. Elias-Miro, J. R. Espinosa, G. F. Giudice, G. Isidori and A. Strumia, JHEP **1208**, 098 (2012) [arXiv:1205.6497 [hep-ph]]; K. Holland and J. Kuti, Nucl. Phys. Proc. Suppl. **129**, 765 (2004) [hep-lat/0308020]; K. Holland, Nucl. Phys. Proc. Suppl. **140**, 155 (2005) [hep-lat/0409112]; Z. Fodor, K. Holland, J. Kuti, D. Negradi and C. Schroeder, PoS LAT **2007**, 056 (2007) [arXiv:0710.3151 [hep-lat]]; P. Gerhold and K. Jansen, JHEP **0907**, 025 (2009) [arXiv:0902.4135 [hep-lat]]; JHEP **1004**, 094 (2010) [arXiv:1002.4336 [hep-lat]].
- [45] G. Aad *et al.* [ATLAS Collaboration], Phys. Lett. B **716**, 1 (2012) [arXiv:1207.7214 [hep-ex]]; S. Chatrchyan *et al.* [CMS Collaboration], Phys. Lett. B **716**, 30 (2012) [arXiv:1207.7235 [hep-ex]].
- [46] S. Rechenberger, Diploma Thesis, Friedrich-Schiller-Universität Jena, March 2010; L. Zambelli, Ph.D. Thesis, Bologna University, January 2013.